Hypoxia and HIF-1 trigger Marek's Disease Virus reactivation in lymphoma-derived latently infected T lymphocytes

Corentin Mallet, Jade Cochard, Sébastien Leclercq, Laëtitia Trapp-Fragnet, Philippe Chouteau, Caroline Denesvre

1   <u>RESEARCH ARTICLE</u>

2   **Hypoxia and HIF-1 trigger Marek's Disease Virus reactivation in lymphomas-derived**

3   **latently-infected T lymphocytes**

4

5   Corentin Mallet[1], Jade Cochard[2], Sébastien Leclercq[1], Laetitia Trapp-Fragnet[1], Philippe

6   Chouteau[2], Caroline Denesvre[1]*

7

8   [1] ISP, INRAE, Université de Tours, 37380 Nouzilly, France

9   [2] INSERM U1259, Université de Tours and CHRU de Tours, France.

10

11   * Corresponding author : Mailing address : Laboratoire de Biologie des Virus Aviaires, INRAE-

12   Université de Tours, UMR1282 ISP, Centre INRAE Val de Loire, 37380 Nouzilly, France.

13   <u>Phone</u> : (+33) 2 47 42 76 19

14   E-mail: <u>caroline.denesvre@inrae.fr</u>

15

16   Running head : Hypoxia triggers MDV reactivation

17   Abstract : 249 words; Importance: 149 words; 10 figures, 3 tables

18

Mallet et al.

19 **ABSTRACT**

20 Latency is a hallmark of herpesviruses, allowing them to persist into their host without

21 virions production. Acute exposure to hypoxia (below 3% O_2) was identified as a trigger of

22 latent-to-lytic switch (reactivation) for human oncogenic gamma-herpesviruses (KSHV and

23 EBV). Therefore, we hypothesized that hypoxia could also induce reactivation of Marek's

24 disease virus (MDV), sharing biological properties with EBV and KSHV (notably oncogenic

25 properties), into lymphocytes. Acute exposure to hypoxia (1% O_2) of two MDV-latently

26 infected cell lines derived from MD tumors (3867K and MSB-1) induced MDV reactivation. A

27 bioinformatic analysis of the RB-1B MDV genome revealed 214 putative hypoxia-response

28 element consensus sequences on 119 open reading frames. RT-qPCR analysis showed five

29 MDV genes strongly upregulated early after hypoxia. In 3867K cells under normoxia,

30 pharmacological agents mimicking hypoxia (MLN4924 and $CoCl_2$) increased MDV

31 reactivation, but to a lower level than real hypoxia. Overexpression of wild-type or stabilized

32 human hypoxia inducible factor-1α (HIF-1α) in MSB-1 cells in normoxia also promoted MDV

33 reactivation. In such conditions, lytic cycle was detected in cells with a sustainable HIF-1α

34 expression, but also in HIF-1α negative cells, indicating that MDV reactivation is mediated by

35 HIF-1, in a direct and/or indirect manner. Lastly, we demonstrated by a reporter assay that

36 HIF-1α overexpression induced the transactivation of two viral promoters, shown

37 upregulated in hypoxia. These results suggest that hypoxia may play a crucial role in the late

38 lytic replication phase observed *in vivo* in MDV-infected chickens exhibiting tumors, since a

39 hypoxic microenvironment is a hallmark of most solid tumors.

40

Mallet et al.   2

41 **IMPORTANCE**

42 Latent-to-lytic switch of herpesviruses (aka reactivation) is responsible for pathology

43 recurrences and/or viral shedding. Studying physiological triggers of reactivation is therefore

44 important for health to limit lesions and viral transmission. Marek's disease virus (MDV) is a

45 potent oncogenic alpha-herpesvirus establishing latency in T-lymphocytes and causing lethal

46 T-lymphomas in chickens. *In vivo*, a second lytic phase is observed during tumoral stage.

47 Hypoxia being a hallmark of tumors, we wondered whether hypoxia induces MDV

48 reactivation in latently-infected T-lymphocytes, like previously shown for EBV and KSHV in B-

49 lymphocytes. In this study, we demonstrated that acute hypoxia (1% O2) triggers MDV

50 reactivation in two MDV transformed T-cell lines. We provide some molecular basis of this

51 reactivation by showing that hypoxia inducible factor (HIF-1) overexpression induces MDV

52 reactivation to a similar extend than hypoxia after 24 hours. Hypoxia is therefore a

53 reactivation stimulus shared by mammalian and avian oncogenic herpesviruses of different

54 genus.

55

56 **KEYWORDS:** Marek's disease virus, reactivation, hypoxia, lymphocytes, HIF-1.

57

58   Herpesviruses are large DNA viruses causing various types of pathologies, in clinical signs and

59   severity, including recurrent local infections and cancers. Such pathologies are associated

60   with the persistence of the virus in the host after infection and its biphasic life cycle, either

61   latent or lytic. The latent cycle consists of a state in which the viral genome persists into the

62   host cell nucleus, with no infectious virions production and a limited number of viral

63   products (either RNA and/or proteins), avoiding detection by the immune system [1]. In

64   contrast, the lytic cycle leads to virions production, cell death, and virus shedding. Each virus

65   species establishes latency in a unique cell type and in a limited number of cells. The

66   identification of the factors and molecular mechanisms governing the switch from latent-to-

67   lytic cycle, named reactivation, is of major importance to limit the recurrence of lesions and

68   viral shedding. Various environmental factors have been identified as triggering reactivation:

69   fever or UV light for herpes simplex virus (HSV-1, aka human herpesvirus 1) [2], and immune

70   system aging for human cytomegalovirus (CMV, aka human herpesvirus type 5) and Epstein-

71   Barr virus (EBV, aka human herpesvirus type 4) [3]. Recently, low oxygen level or hypoxia (≤

72   3%) was identified as a potent reactivation factor for gamma-herpesviruses. Initially

73   demonstrated for the Kaposi sarcoma-associated virus (KSHV, aka human herpesvirus type

74   8) in B cells [4], hypoxia was also shown to induce the reactivation of two other gamma-

75   herpesviruses in B-cells, EBV and the murine herpesvirus type 4 (MHV-4) [5, 6]. For these

76   three viruses, the hypoxia inducible factor 1 (HIF-1) was shown as a molecular determinant

77   triggering reactivation, by turning-on the expression of at least one critical gene in the

78   initiation of the lytic cycle: BZLF-1 for EBV [5, 7], ORF50-rta for KSHV [8, 9] and MHV-4 [6].

79   HIF-1 is a transcription factor whose activity is tightly regulated by oxygen [10]. HIF-1 is a

80   heterodimer constituted of two sub-units, HIF-1α and HIF-1β, found in the entire animal

81   kingdom [11]. HIF-1 protein regulation is based on HIF-1α degradation or stabilization,

82 depending on the percentage of oxygen. In normal oxygen conditions (normoxia; 21%, v/v),

83 HIF-1α is quickly degraded by the proteasome after hydroxylation of three amino acids

84 (Pro402, Pro564, Asn803), Von Hippel Lindau (VHL) binding, and ubiquitinylation (reviewed

85 in [10, 12]). In normoxia, HIF-1α half-life is below 5 minutes [13]. In hypoxia, the prolyl-4-

86 hydroxylases modifying HIF-1α are non-functional [14] and HIF-1α is stabilized [15].

87 Stabilized HIF-1α is subsequently translocated into the nucleus, where it dimerizes with the

88 constitutively expressed HIF-1β subunit leading to an active HIF-1. The HIF-1 heterodimer

89 then binds to hypoxia response element sequences (HREs) located within the promoter of

90 target genes, leading to their transcription. HIF-1 target genes are involved in metabolism

91 (lipids, carbohydrates), angiogenesis, erythropoiesis, and their expression allows an adaption

92 to low oxygen conditions at cell, tissue, or organism level [10].

93 Marek's disease virus (MDV, aka Gallid herpesvirus type 2), is an alpha-herpesvirus from the

94 Mardivirus genus that causes immunosuppression and lethal T- lymphomas in chickens.

95 After entry through the respiratory tract, MDV infects B- and T-lymphocytes causing an early

96 cytolytic infection, between 3 and 7 days post-infection (dpi) [16, 17]. At about 7 dpi, MDV

97 establishes latency in a subset of T-lymphocytes, mostly CD4-positive [18], and its genome

98 integrates into the host's genome telomeres [19-21]. During latent infection, a few MDV

99 products are expressed: the Meq oncoprotein [22], several non-coding latency associated

100 transcripts (LATs) [23, 24] as well as several micro RNAs (miRNAs) [25, 26]. Latent infection

101 in T-cell is considered necessary for MDV transformation, which occurs 3 to 4 weeks post-

102 infection. According to Calnek's model [18], a second lytic cycle called 'late cytolytic

103 infection' occurs in lymphoid organs at a later time post-infection, when tumorigenesis is

104 already established. MD tumors have been shown to contain 0.1% of CD4+ T-cells in lytic

105 cycle [27], probably due to the reactivation of MDV. The stimuli triggering MDV reactivation

106 in lymphoid organs and tumors *in vivo* are still poorly known [28]. Hypoxia has been

107 depicted as a common feature in solid tumors' microenvironment [29], notably when

108 tumors cells rapidly proliferate, resulting in poor oxygen supply in the center of the tumor

109 due to a lack of vascularization [30, 31]. Although hypoxia has not been demonstrated in

110 Marek's disease (MD) T-lymphomas yet, we assumed that hypoxia exists in MD tumors due

111 to their extremely rapid growth in chickens. By analogy with what has been reported for

112 gamma-herpesviruses, we wondered whether hypoxia may contribute to MDV reactivation

113 in MD lymphomas. In this study, our aim was to explore whether hypoxia can induce MDV

114 reactivation in latently-infected T-cells. To this end, we used two well characterized cell lines

115 established from MD lymphomas, MSB-1 [32, 33] and 3867K [34]. We show for the first time

116 that hypoxia (1% O_2) induces MDV reactivation in T-cell lines *in vitro*. Using overexpression

117 of HIF-1α in normoxia, we show that this transcription factor plays a crucial role in MDV

118 reactivation. Altogether these findings provide new insights on MDV reactivation

119 mechanisms.

120

121 **RESULTS**

122 ***Hypoxia increases the proportion of 3867K cells in lytic cycle.***

123 To determine whether hypoxia can induce MDV reactivation, we used a T- lymphoid cell line

124 latently-infected with the very virulent recombinant RB-1B 47eGFP, the 3867K cell line [34].

125 When virus reactivates, the lytic pUL47eGFP tegument protein is expressed, allowing the

126 detection of GFP-positive cells [34, 35]. To start, 3867K cells were cultivated either in

127 normoxia (at 21% O_2) or in hypoxia (at 1% O_2) for 72 hours (h). Viral reactivation was

128 measured by flow cytometry by determining the percentage of GFP-positive cells in live cells.

129 Under normoxic condition, the live GFP-positive cells represented 0.85% of the total cells

130 (Fig. 1A, left panel), corresponding to spontaneous reactivation. In hypoxia, live GFP-positive

131 cells increased to 4%, i.e. 4.7-fold compared to normoxic conditions (Figure 1A, right panel).

132 In both conditions, EGP-positive cells mean fluorescence was relatively low (about 70 in

133 arbitrary units) (vs 5 to 10 arbitrary units in latently-infected cells), consistent with the low

134 expression of pUL47eGFP during the lytic cycle in lymphocytes. In addition, the cellular

135 mortality increased upon hypoxia (eFluor 780-positive cells), with dead cells representing

136 51.8 % of the total cells in hypoxia compared to 12.5% in normoxia (Figure 1A).

137 To confirm that the expression of pUL47eGFP reflected the switch to lytic cycle and not just

138 a transcriptional activation of *UL47eGFP* expression under hypoxia, we verified by

139 fluorescence microscopy the expression of two other late viral proteins essential for MDV

140 infectivity: the major tegument protein VP22 and glycoprotein B (gB). Both VP22 and gB

141 were expressed in nucleated GFP-positive cells, with similar localization in normoxia and

142 hypoxia, consistent with the fact that pUL47eGFP-positive cells underwent a lytic cycle in

143 both conditions (Figure 1B). In hypoxia, we noticed numerous cells emitting a low green

144 fluorescence signal devoid of nucleus (Hoechst-negative), cells which were not stained for

145 VP22 or gB (Figure 1B). Such cells were absent when viable cells (efluor 780-negative) were

146 cell-sorted by flow cytometry before VP22 antibody staining (Figure 1C and below).

147 Therefore, these enucleated green cells correspond most likely to a subpopulation of dead

148 cells with an increased autofluorescence intensity and not to viral reactivation prior to cell

149 death.

150 We next determined whether MDV reactivation was time-dependent under hypoxia. To this

151 end, 3867K cells were cultivated in normoxia or hypoxia for 96 h and the percentage of

152 reactivation was estimated every 24 h through pUL47eGFP expression by flow cytometry.

153 While the percentage of live GFP-positive cells among live cells remained low in normoxia at

154   every time points (≤2%), it increased progressively approximatively 4-fold in hypoxia, from

155   2.5% to 9.5% between 24 and 96 h (Figure 1D). Cell mortality was between 12% and 25% in

156   normoxia and between 32% and 66% in hypoxia (Table 1).

157   To further confirm that cells reactivating MDV under hypoxia are fully MDV productive, we

158   determined the number of MDV genome copies per cell by quantitative PCR (qPCR) under

159   normoxic and hypoxic conditions during 96 h (Figure 1E). In normoxia, the MDV genome

160   copy number was below 5×10^7 per 10^6 cells at all time points tested, corresponding mostly

161   to viral genomes integrated into the host genome. In hypoxia, MDV genome copy number

162   per 10^6 cells increased progressively approximatively 4-fold. Such increase demonstrates

163   that MDV reactivation in hypoxic cells is associated with an increased production of MDV

164   genomes in these cells.

165

166   **Hypoxia increases viral lytic genes expression in 3867K T-cell line, notably *ICP4*, *ICP27*,**

167   ***UL39*, *UL41* and *UL49*.**

168   In order to study the effect of hypoxia on viral genes expression, we next performed a bio-

169   informatic analysis on the complete RB-1B genome to locate and enumerate all putative

170   HREs in the promoter area of each identified open reading frame (ORF) (incl. hypothetical

171   ones). In total, we identified 214 putative HREs on 119 ORFs (140 ORFs having been

172   estimated on this genome [36]). The number of predicted HREs per promoter varied from 1

173   to 5, at the most. Note that *UL47*, *UL49* encoding VP22, and *UL27* encoding gB showed 1, 3,

174   and no HRE respectively. Among MDV genes we selected sixteen lytic genes, thirteen with

175   putative HREs and three without (Figure 2A): two immediate early (IE) genes (*ICP4* and

176   *ICP27*), five early (E) genes (including *UL39* encoding the ribonucleotide reductase large sub-

177   unit (RR1) and *UL41* encoding the viral host shutoff protein (VHS)) and nine late (L) genes

178 (including *UL47*, *UL49*, and *UL27*). *UL13*, *UL27*, and *UL48* are devoid of HRE in the promoter

179 area analyzed.

180 We assessed the effect of hypoxia on the expression of these sixteen viral transcripts

181 encoding lytic proteins by reverse transcriptase qPCR (RT-qPCR) over a 72-h period. The

182 expression of *Meq*, which is expressed in both latent and lytic phases was also quantified. Of

183 these seventeen genes, eleven (including UL47) were slightly upregulated (3- to 7-fold) 24 h

184 after hypoxia compared to normoxia, while five were greatly upregulated: the two IE genes,

185 *ICP4* and *ICP27* were upregulated 18- and 16-fold, respectively; two E genes, *UL39* and *UL41*

186 were upregulated 28- and 12-fold, respectively; and one L gene, *UL49*, was upregulated 17-

187 fold (Figure 2B). The high expression of *UL49* at that time point was striking. At 48 h of

188 hypoxia, all sixteen lytic genes (IE, E, and L) showed a mRNA expression at least 10-fold

189 higher (between 11- and 31-fold) than in normoxic conditions. At 72 h of hypoxia, the

190 expression of all lytic genes was still high, between 11- and 60-fold that of normoxia. At that

191 time, *ICP4*, ICP27, *UL39*, *UL41*, and *UL49* were still the most upregulated genes (> 40-fold),

192 like at 24 h. At 48 and 72h of hypoxia, *US7* encoding gI was also found highly upregulated.

193 The six most upregulated genes contain at least one HRE upstream (-) or downstream (+) of

194 their starting codon, which are strictly conserved in Md5 genome, another very virulent

195 MDV strain: *ICP4* (+49), *ICP27* (-165), *UL39* (-396, -654), *UL41* (-106, -356), *UL49* (-136, -285, -

196 301), and *US7* (-15, -90, -105). Note that *meq* expression was increased but less than all lytic

197 genes at 48 and 72h. All together, these results show that hypoxia induced the expression of

198 all viral lytic genes assessed, with a few genes upregulated, most likely via HRE.

199

200 ***MDV reactivation induced by hypoxia is not restricted to a cell line or a MDV genotype.***

201 To investigate whether hypoxia-induced reactivation is restricted to the 3867K cell line

202 and/or to the RB-1B virus, we examined the effect of hypoxia on the most frequently used

203 MD derived-cell line (MSB-1) obtained with the virulent BC-1 MDV strain, and whose

204 reactivation is not traceable with a fluorescent gene. Therefore, to monitor MDV

205 reactivation, we first quantified MDV genome copy numbers under normoxic and hypoxic

206 conditions over a 96-h period (Figure 3A). The number of MDV genome copies per million

207 cells was below 5×10^7 at all time points under normoxia. It increased from 4.6×10^7 at 24 h

208 to 2.7×10^8 at 96 h under hypoxia. The fold-changes between hypoxia and normoxia

209 increased over time, except for an inflection point at 72 h (which is probably due to a high

210 mortality recorded in hypoxia starting at 48 h) (Table 1). This tumoral cell line also exhibited

211 a high rate of mortality, even in normoxic condition (between 25% and 44%) (Table 1).

212 Reactivation was next verified by examining the expression of VP22 after antibody staining

213 by fluorescence microscopy (Figure 3B). A strong VP22 signal was visible in the cytoplasm of

214 cells, much more frequently in hypoxia than in normoxia at 24 and 48 h. Numerous

215 apoptotic nuclei were visible in normoxia and hypoxia, in accordance with the high mortality

216 (as reported above). By counting VP22-positive cells among all cells exhibiting non-apoptotic

217 nucleus by fluorescence microscopy, we estimated the % of MSB-1 reactivation at 3.2% and

218 7.3% after 24 h and 48 h of hypoxia, respectively, compared to < 1% in normoxia at both

219 time points.

220 To confirm that viral reactivation was indeed induced by hypoxia in MSB-1, we quantified

221 mRNA expression of sixteen lytic genes as well as *meq* by RT-qPCR as performed earlier for

222 3867K. The fold-changes between hypoxic and normoxic conditions are shown in Figure 3C.

223 At 24 h of hypoxia, only *UL39* and *UL49* were upregulated > 10-fold compared to normoxia,

224 while the other genes were upregulated 2- to 5-fold. At 48 h of hypoxia, all genes were

225   expressed > 10-fold (between 14 and 74-fold), with *ICP4*, *UL39*, *UL41*, *UL49*, and *US7* being

226   the most upregulated (≥ 35-fold). This was similar to that observed in 3867K cells except that

227   the fold-changes were globally higher at that time point (48 h) in MSB-1 than in 3867K. At 72

228   h of hypoxia, a gene expression for all genes was lower than at 48 h, as observed for DNA

229   genome copies.

230   Therefore, acute hypoxia induced MDV reactivation in both MSB-1 and 3867K cell lines alike,

231   although MSB-1 cells showed a higher viral gene expression and mortality compared to

232   3867K.

233

234   ***Hypoxia induces MDV reactivation in HIF-1α-positive cells and activates the expression of***

235   ***HIF-1 cellular target genes.***

236   Among HIFs, HIF-1α is the major cell regulator in hypoxia and the most ubiquitous. HIF-1α

237   has been shown to trigger viral reactivation in hypoxic conditions in three gamma-

238   herpesvirus [4-6]. To investigate the role of HIF-1α in MDV reactivation during hypoxia, we

239   first studied the expression of HIF-1α in 3867K and MSB-1 grown under hypoxia compared

240   to normoxia by fluorescence microscopy. To this end, both cell lines were grown in both

241   conditions for 48 h and live cells were sorted by flow cytometry before staining. The chicken

242   HIF-1α protein was detected by immunofluorescence, whereas virus reactivation was

243   detected with pUL47eGFP expression for the 3867K cell line and after VP22 immunostaining

244   for MSB-1 cells. Note that in these conditions, all 3867K cells emitting green fluorescence

245   have a nucleus (Figure 4). In normoxia, HIF-1α was almost undetectable in both 3867K and

246   MSB-1, indicating that HIF-1α was not stabilized in these transformed T-cells (Figure 4A-B,

247   upper panels). In contrast, in hypoxia, almost all 3867K and MSB-1 cells were HIF-1α-positive

248   as expected when this protein is stabilized (Figure 4A-B, lower panels). The quantification of

249   the HIF-1α signal per cell confirmed that the fluorescence intensity was significantly higher

250   in hypoxia than in normoxia in both cell lines, although weak notably in 3867K (Figure 4 C-D).

251   These results indicated that HIF-1α was indeed stabilized in both cell lines cultivated under

252   hypoxia. In hypoxia, among HIF-1α-positive cells, only a fraction of the live cells was

253   expressing lytic viral proteins as earlier.

254   To verify that HIF-1α stabilization under hypoxia was functional in MDV T-cell lines, we

255   examined HIF-1 transcriptional activity by measuring the expression of three HIF-1 cellular

256   target genes identified for mammals [10]: *GLUT1*, the glucose transporter 1; *LDHA*, the

257   pyruvate dehydrogenase A which mediates the conversion of pyruvate in lactate; and *iNOS*,

258   the inducible nitric oxide synthetase. Cells (3867K and MSB-1) were cultivated under hypoxia

259   or normoxia for 72 or 96 h and the mRNA levels of *GLUT1*, *LDAH*, and *iNOS* were measured

260   by RT-qPCR every 24 h. In 3867K cells, all three genes were upregulated under hypoxia

261   compared to normoxia at all time points (Figure 5A). Most fold-changes ranged between 5

262   and 15. We also verified in the same manner, that HIF-1 was functional in MSB-1 cells

263   cultivated in hypoxia (Figure 5B). Taken together, we demonstrated that HIF-1α was

264   stabilized under hypoxia exposure in both 3867K and MSB-1 cell lines and that HIF-1 was

265   functional.

266

267   ***Hypoxia-mimicking pharmacological agents CoCl₂ and MLN4924 induce MDV reactivation***

268   ***in 3867K cells.***

269   To study the specific role of HIF-1α stabilization in MDV reactivation, we tested two

270   pharmacological agents, MLN4924 and CoCl₂, known to stabilize HIF-1α in mammalian cells

271   in normoxia by reducing its degradation. 3867K cells were cultivated in the presence of each

272   drug at different concentrations for 24 h in normoxia (two independent experiments). MDV

273   reactivation and cell mortality were assessed by flow cytometry as described earlier. Both

274   drugs increased MDV reactivation in a dose-dependent manner compared to mock-treated

275   cells as negative control (Figure 6A). The mortality observed with MLN4924 and CoCl$_2$ at the

276   upper doses was 22.85% and 14.1%, respectively. Cells were treated with sodium butyrate

277   (0.5 mM for 48 h), an inhibitor of histone deacetylases, as positive control of reactivation,

278   leading to a 5.3-fold increase of reactivated live cells (with a mortality of 18.6% of total

279   cells). CoCl$_2$ treatment (250 μM) led to a 2.3-fold increase of reactivated live cells compared

280   to control. MLN4924 treatment at 1 and 2.5 μM induced a greater reactivation, with 3.7-

281   and 4.2-fold increase, respectively. MLN4924's effect was time-dependent since no

282   reactivation was observed with 1 μM after 8 h of treatment compare to control. MDV

283   reactivation being milder with CoCl$_2$ than with MLN4924 treatment, subsequent analyses

284   were only performed with MLN4924. We next examined HIF-1α and MDV lytic antigens

285   expression by fluorescence microscopy on 3867K cells treated with 1 μM MLN4924 for 24 h.

286   HIF-1α was detected in most MLN4924-treated cells including reactivating MDV cells but not

287   in DMSO-treated cells (control) (Figure 6B). To confirm reactivation, the RNA expression of

288   four lytic genes (*ICP4*, *UL39*, *UL49*, and *UL13*) was measured by RT-qPCR and compared to

289   DMSO-treated cells. The expression of all four viral genes increased as expected in two

290   independent experiments (Figure 6C). Next, we examined the activity of HIF-1 by measuring

291   the mRNA expression of two cellular HIF-1 targets (*LDAH* and *GLUT-1)*. Surprisingly the

292   expression of these two genes did not change compared to the DMSO control. All together,

293   these results showed that MLN4927 induces MDV reactivation in 3867K cells, but the role of

294   HIF-1α stabilization in that process could not be clearly demonstrated. The way by which

295   MLN4924 may induce MDV reactivation herein is discussed later.

296

297   ***Human HIF-1α is functional in chicken cells.***

298   To further clarify the role of HIF-1α in MDV reactivation and in absence of validated chicken

299   HIF-1α tools, we verified the functionality of the human HIF-1α (hHIF-1α) in chicken cells

300   after transient transfection with expressing vectors. Lymphocytes are cells known to be

301   extremely difficult to transfect with plasmids. Therefore, we first optimized the transfection

302   efficiency by using the Neon® nucleofector technology, a technology which allows high

303   transfection efficiency with human lymphocytes. An orange fluorescent reporter plasmid

304   (pPB tdTomato) of large size (8.67kb) was used for that purpose. At 24 h post-transfection,

305   transfection efficacy was 6.7% in 3867K cells and 24.7% in MSB-1 cells, based on Tomato-

306   fluorescence using flow cytometry.

307   We next studied the functionality of hHIF-1α in MSB-1 cells, which gave the higher rate of

308   transfection. To this end, we used two hHIF-1α: the hHIF-1α WT or a stabilized mutant

309   (hHIF-1α mut). This mutant has three amino-acids mutated to prevent its hydroxylation and

310   subsequent degradation in the presence of a high-rate of oxygen (*ie,* 21%). It is therefore

311   stabilized in normoxia in contrast to the WT which is degraded by the proteasome. Using

312   Neon® technology, MSB-1 cells were transfected with the pHRE-d2EGFP reporter plasmid

313   and a vector expressing hHIF-1α (mut or WT). When HIF-1α is expressed at a sufficient level,

314   the eGFP reporter gene is expressed. The pHRE-d2EGFP plasmid encodes a destabilized

315   eGFP, with a short half-life of 2 h, under the control of a minimal promoter containing 5 HRE

316   sequences. Due to its destabilization, the eGFP visualized in cells is therefore the result of

317   recently synthetized proteins and not the result of accumulated proteins overtime. The eGFP

318   expression was monitored by fluorescence microscopy at 8, 24, and 48 h post-transfection

319   (Figure 7). In hHIF-1α mut-expressing cells, the percentage of GFP-positive cells was at the

320   highest (28.5 %) at 24 h post-transfection (Figure 7A). Note that this percentage is consistent

321   with the % of transfection that we measured with the pPB tdTomato. The % of GFP-positive

322   cells decreased at 48 h (13.1%), probably due to the resuming of cell division and the

323   increase of non-transfected cells. In the absence of hHIF-1α mut (pHRE-d2EGFP only), the

324   percentage of GFP-positive cells was < 4.2% at all time points. These data indicate that hHIF-

325   1α mut transactivates a minimal promoter harboring (5 x) HRE in MSB-1. With the hHIF-1

326   WT, the percentage of GFP-positive cells was of 7.1% at 24 h post-transfection (Figure 7B),

327   which is much less than with hHIFα mut as expected. This indicates that, when

328   overexpressed, hHIF-1α WT is also capable of transactivating a promoter with HREs, but to a

329   lesser extent than the hHIF-1α mut. Altogether, these data show that the human HIF-1α (WT

330   or stabilized) is functional in chicken T-cells, indicating that it can dimerize with the avian

331   HIF-1ß. Additionally, we demonstrated for the first time that the Neon technology provides

332   good transfection rates in an avian lymphoid cell line.

333

334   ***HIF-1α overexpression triggers MDV reactivation in MSB-1 cells.***

335   To determine whether HIF-1α could play a role in MDV reactivation, hHIF-1α (mut or WT)

336   was overexpressed in MSB-1 cells cultured in normoxia. To this end, MSB-1 cells were

337   transfected with either expression vector and were examined 24 h post-transfection by

338   fluorescence microscopy after immunostaining for HIF-1α and MDV lytic antigens. The

339   percentage of HIF-1α-positive cells was 13% and 3.8% with hHIF-1α mut and WT,

340   respectively (Figure 8A). This suggested a "mild" stabilization of HIF-1α in the cells

341   transfected with hHIF-1α WT and a greater stabilization in the cells transfected with hHIF-1α

342   mut, as previously observed in Fig. 7. Note that the detection of HIF-1α by

343   immunofluorescence is less sensitive of 13 to 21% at detecting HIF-1α expression than with

344   the reporter gene assay. Therefore, the percentage of HIF-1α-positive cells may be slightly

345 underestimated herein. The percentage of MDV reactivation was then evaluated by counting

346 the relative number of ICP4/VP22-positive cells. The percentage of reactivated cells was

347 about 3% with both hHIF-1α WT and mut and < 1% with the empty pcDNA3 (0.5%) and non-

348 transfected cells (0.7%) (Figure 8B). This indicates that not all cells expressing HIF-1α

349 reactivated, as observed earlier in hypoxic condition.

350 We next examined whether MDV reactivation occurs only in cells in which HIF-1α is

351 detectable. To this end, the percentage of cells expressing both HIF-1α and MDV antigens

352 (VP22/ICP4) were counted by fluorescence microscopy (Figure 8C and D). The % of double-

353 labelled cells was 0.9% with HIF-1α mut and of 0.2% with HIF-1α WT (Figure 8C). Therefore

354 surprisingly > 2% of reactivated cells were *not* HIF-1α-positive. These results demonstrate

355 that HIF-1α mutant and WT expression triggers MDV reactivation. They also suggest a direct

356 and/or indirect effect of HIF-1α on MDV reactivation, discussed below.

357

358 ***HIF-1α over-expression activates MDV UL39 and UL49 viral promoters.***

359 To further explore the molecular mechanism by which hypoxia induces MDV reactivation,

360 we examined if the stabilized hHIF-1α can transactivate the promoters of the five MDV lytic

361 genes, that we found upregulated in hypoxia (ICP4, ICP27, UL39, UL41 and UL49) (Figure 2A).

362 For that, we cloned the five HRE-containing promoter regions of these genes upstream of a

363 destabilized firefly luciferase (fLuc), as well as two MDV promoters (UL36, UL45) devoid of

364 HRE as controls. The promoter constructs were transfected in ESCDL-1 chicken cells in

365 normoxia, with or without the stabilized hHIF-1α vector. A Renilla Luciferase plasmid (pRL)

366 was also co-transfected to standardize the transfection efficiency. At 24 h post-transfection,

367 the expression of the stabilized hHIF-1α was verified (Figure 9A) and the relative luciferase

368 activity (ratio of the fLuc/RL) was calculated (Figure 9B). In absence of the stabilized hHIF-1α,

369 the basal activity of each promoter was low (relative luciferase activity <0.5). The ectopic

370 expression of the stabilized hHIF-1α induced a significant increase of the transcriptional

371 activity for all promoters. Despite this increase, the promoter activity of ICP4, ICP27 and

372 UL41 remained low (0.13, 0.03, 0.16, respectively) at a level similar to the negative control

373 promoters (0.27 and 0.15 for UL36 and UL45, respectively). In contrast, the promoter activity

374 of UL39 and UL49 reached high levels (3.5 and 5, respectively). These results indicate that

375 the ectopic overexpression of HIF-1α is sufficient to transactivate UL39 and UL49 promoters

376 and to induce a strong expression of a reporter gene, but insufficient to efficiently

377 transactivate ICP4, ICP27 and UL41 promoters.

378

379 ***Caspase 3/7-mediated apoptosis observed in hypoxia does not promote MDV reactivation.***

380 HIF-1 was involved in the regulation of apoptosis pathways [37] and caspase activities was

381 shown to promote latent-to-lytic switch and/or viral replication [38]. Therefore, we next

382 explored whether the apoptosis induced under hypoxia could favor MDV reactivation

383 indirectly through caspases activation. We focused on caspase 3, a final effector in apoptotic

384 death. First, we validated Z-DEVD-FMK as a caspase 3 inhibitor on 3867K cells, showing

385 "physiological" apoptosis in normoxia (Table 1), using the luminescent Caspase-Glo® 3/7

386 assay. 3867K cells treated with 50μM of Z-DEVD-FMK for 24 h in normoxia showed a caspase

387 3/7 activity significantly reduced of 92.5-fold compared to in its absence (Figure 10A). Next,

388 3867K cells were cultivated in hypoxia for 72 h in presence or absence of Z-DEVD-FMK

389 (50μM), with Z-DEVD-FMK renewal every 24 h. After 48 h and 72 h, caspase 3/7 activity was

390 assayed in parallel to cell mortality and MDV reactivation by flow cytometry as previously

391 used. In the presence of Z-DEVD-FMK under hypoxia, the caspase 3/7 activity was

392 significantly reduced of 135-fold at 48 h and of 421-fold at 72h (Figure 10B). At 48h,

393 reactivated cells (GFP-positive cells) represented 4.1% of the live cells treated with Z-DEVD-

394 FMK, close to the 3.4% measured for Z-DEVD-FMK-untreated cells (Figure 10B, left panel). At

395 72 h, the percentage of GFP-positive cells raised up to 6.4% with Z-DEVD-FMK, a rate

396 comparable to the 5.4% observed without Z-DEVD-FMK (Figure 10B, right panel). The results

397 thus indicate that MDV reactivation upon hypoxia is not promoted by caspase 3/7 activity in

398 the 3867K cell line.

399

400 **DISCUSSION**

401 This is the first study showing that acute hypoxia launches MDV lytic cycle from

402 latently infected T-lymphocytes derived from MD-lymphomas. Previous studies

403 had shown a reactivation effect of hypoxia on gamma-herpesviruses from latently

404 infected B-cells [4-6]. Here we showed the reactivation of an alpha-herpesvirus,

405 indicating that hypoxia may be a reactivation stimulus shared by several

406 herpesvirus subfamilies. As for most herpesviruses, EBV, KSHV, and MHV-4 persist

407 as episome in latency [39], whereas MDV integrates in the cellular genome,

408 preferentially in the telomeres [19-21]. Therefore, having a latent episomal form is

409 not a condition necessary for herpesvirus reactivation by hypoxia. In this study, we

410 detected reactivation only in a subset of the cells exposed to hypoxia or treated

411 with chemicals stabilizing HIF-1α in normoxia. This result is consistent with

412 previous reports on gamma-herpesviruses. Indeed, Davis et al. reported less than

413 3% KSHV-reactivating cells among BC-3 and BCBL-1 exposed to 1% O_2 during 48 to

414 72 h [4]. Polcicova et al. reported a much higher reactivation rate (52%) for MHV-4

415 from NB-78 cells exposed to 2% O_2 for 72 h [6]. However, these cells also exhibited

416 an unusual spontaneous reactivation level of 7%. Kraus et al. also reported EBV

417   reactivation in a subset of HIF-1α -positive cells treated with deferoxamine (DFO),

418   an agent mimicking hypoxia like MLN4924 [7]. In addition, this feature of partial

419   reactivation was also observed when MD derived T-cells were treated *in vitro* with

420   pharmacological agents acting through different mechanisms, for instance

421   modifications of the chromatin structure (*eg,* with sodium butyrate) [40],

422   alterations of DNA integrity, or replication (*eg,* with etoposide, 5-

423   iododexoxyuridine) [41, 42]. Why all the cells in a "clonal" population do not

424   reactivate after exposure to a reactivation stimulus is currently unknown. Single-

425   cell RNA sequencing may enable answer this question.

426   Herein, virus reactivation was detected based on viral lytic genes expression and

427   viral DNA quantification, as always performed for MDV. Because MDV replication

428   in culture results only in 0.1% intracellular mature virions in 3867 K [34] with no

429   extracellular virions detectable, we could not measure whether reactivation in

430   hypoxia led to a productive cycle with mature virions.

431   Besides reactivation, hypoxia was associated with high cell mortality, particularly with

432   MSB-1 cells. Such mortality levels were unexpected because hypoxia is a hallmark of most

433   human solid tumors [29], including lymphomas [43]. Depending on the cell type, hypoxia

434   can have opposing effects on cell death, especially apoptosis [44]. While numerous cells

435   establish apoptosis protection mechanisms when exposed to hypoxia [45], some remain

436   sensitive to apoptosis. For example, hypoxia induces apoptosis in the human oral

437   squamous cell carcinoma cell line (OSC-4) [46] and in primary rat fibroblasts transformed

438   by Ras and Myc oncogenes [47]. Therefore, one can wonder if the phenotype observed

439   herein with MSB-1 and 3867K cell lines is peculiar to these cell lines or a common feature

440   of MD-lymphomas derived cells. In our study, four possible mechanisms may have

441 contributed to cell death in hypoxia: first, hypoxia may have caused a global metabolic

442 and oxidative cellular stress due to a lack of ATP, mitochondria damages, or reactive

443 oxygen species [ROS] production. Hypoxia triggers HIF-1 stabilization, which is known to

444 activate NOX and iNOS genes [48], potentially leading to apoptosis [49]. Second, hypoxia

445 may have caused a glucose/nutrient shortage, which is highly toxic for cells [50]. Because

446 the medium was not renewed during the 72-96 h of hypoxia, we cannot rule out that cells

447 had consumed most of the glucose/nutrients, and had lacked glucose/nutrients in

448 addition to O_2 at some time points. Third, hypoxia may have caused the premature

449 expression of a viral cytotoxic protein. Indeed, UL49, considered a 'late' viral gene was

450 upregulated after only 24 h of hypoxia. UL49 encodes VP22, a tegument protein essential

451 for MDV replication that triggers DNA damage in proliferating cells when ectopically

452 expressed [51]. Fourth, the lytic cycle itself could have led to cell death, notably at 72 and

453 96 h. This last hypothesis is the less probable as sorted-dead cells did not express lytic

454 antigens after 48h in hypoxia as shown in figure 1C.

455 We observed MDV reactivation in normoxia in 3867K cells with $CoCl_2$ and MLN4924, two

456 molecules known to mimic hypoxia in numerous mammalian cells by stabilizing HIF-1α.

457 Treatment with these chemicals for 24 h induced 2- to 4-fold MDV reactivation compared

458 to mock-treated cells. This is comparable to the level of KSHV reactivation (5-fold, based

459 on gpK8.1 lytic protein expression) in BCBL-1 treated with 100 mM $CoCl_2$ for 72 h [4]. EBV

460 reactivation into lytic infection and HIF-1α stabilization has been reported with various

461 hypoxia mimicking molecules, including MLN4924, in the EBV+ GV-derived cell lines [7].

462 Although HIF-1α was detected (albeit at a low level) in all MLN4924-treated cells, it

463 remains unclear whether MDV reactivation was due to HIF-1 stabilization. Indeed, we did

464 not observe an upregulation of the HIF-1 glycolytic target genes, suggesting that HIF-1

465 may not be sufficiently expressed or was missing a cofactor (for *e.g.* p300/CBP) to be fully

466 functional [52]. Thus we suspect that the reactivation observed with MLN4924 could also

467 be independent of HIF-1α. MLN4924 is known to induce deregulation of the S-phase DNA

468 synthesis in tumoral cells with rapid cell division [53] and induce DNA double-strand

469 breaks (DSBs) [54]. As we have previously shown that induction of DNA DSBs triggers

470 reactivation in 3867K cells [42], we suspected that the reactivation with MLN4924 could

471 also be due to this molecular mechanism.

472 We demonstrated that hHIF-1α is functional in two chicken cell lines when overexpressed.

473 Our result therefore indirectly indicates that the hHIF-1α can dimerize with the chicken HIF-

474 1ß. Nevertheless, despite the HRE conservation in vertebrates and the high amino acid

475 identity of 79% between the chicken and human HIF-1α proteins [55], it cannot be certified

476 that hHIF-1α is fully as efficient as its chicken counterpart for MDV reactivation.

477 Although we clearly demonstrated that HIF-1α expression triggers MDV reactivation in

478 MSB-1 cells, the molecular pathway initiating MDV reactivation remains puzzling. Ectopic

479 expression of hHIF-1α (WT and stabilized) led to reactivation of 3.25% of the cells 24 h

480 post-transfection, which is consistent with the percentage of MSB-1 cells reactivated after

481 24 h under hypoxia (3.16%). However, the fact that HIF-1α WT led to the same

482 reactivation efficacy than the stabilized HIF-1α mutant is surprising, because HIF-1α WT

483 was less effective than the stabilized HIF-1α at transactivating the reporter gene (EGFP

484 destabilized protein). One possible explanation is a 'hit-and-run' mechanism, whereby WT

485 HIF-1 is expressed, triggering the lytic cycle in some cells, but its too transient expression

486 makes it undetectable at the time of cell fixation. A similar observation was made in EBV+

487 GC derived-cells treated with DFO for 24 h; after DFO removal, cells had lost HIF-1α

488   expression but were still in lytic cycle [7]. Another unexpected result was that only 0.9%

489   and 0.2% of the reactivated cells were HIF-1α-positive by immunofluorescence after

490   transfection with stabilized or WT HIF-1α, respectively. Although these percentages are

491   possibly slightly underestimated (immunofluorescence being less sensitive at detecting

492   HIF-1α expression than the reporter assay), this result indicates that the effect of HIF-1 on

493   reactivation may be direct and/or indirect. If here again a hit and run mechanism can be

494   possible, another plausible hypothesis is an indirect effect of HIF-1. Indeed, HIF-1 is known

495   to activate more than 100 cellular genes in mammals [56], including secreted proteins and

496   adhesion molecules. In addition, hypoxia and HIF-1 stimulate the production of cellular

497   exosomes and modify their contents [57]. Therefore, one or several cellular components

498   released in the extracellular environment during hypoxia may play a "pro-reactivation"

499   role on the neighboring cells.

500   During hypoxia, MDV reactivation was accompanied by an increased transcription of all

501   sixteen lytic genes monitored, some of which exhibiting putative HREs in their promoter

502   regions. Among these sixteen lytic genes, six were overexpressed both in 3867K and MSB-

503   1 under hypoxia, which makes them susceptible to be targeted by HIF-1. The presence of

504   1 to 3 HREs in the promoter region of these six genes in RB-1B and Md5 is consistent with

505   this interpretation. The fact that only a few genes harboring one or several HREs are

506   overexpressed in hypoxia is not surprising. Indeed, in mammalian cells, only 1% of the

507   cellular HREs were found to bind HIF-1 by chip assay after hypoxia exposure [56].

508   In gamma-herpesviruses, a single IE gene regulates the latent-to-lytic switch: ORF50-rta

509   for KSHV and MHV-4 and BZLF1 for EBV. These genes are transcriptionally activated by

510   HIF-1 [6-9]. We reasoned that this molecular mechanism could also trigger MDV

511   reactivation in hypoxia. In that perspective, *ICP4* is of particular interest as it is considered

512 as a potential initiator of the lytic cycle, although this has not been demonstrated. Our

513 data from the promoter assay showed that the overexpression of the stabilized hHIF-1α in

514 normoxia increases the basal activity of the ICP4 promoter, but which remained low, close

515 to the basal activity of promoters lacking HRE. This result suggests that the upregulation

516 of ICP4 observed in hypoxia is independent of the HRE present in its promoter and might

517 rely on other cellular or viral factors induced upon hypoxic conditions. Interestingly the

518 promoter assay showed a clear upregulation of UL39 and UL49 promoters activity by HIF-

519 1, which is in accordance with the transcripts expression after 24h of hypoxia in both cell

520 lines. How UL39 expression could contribute to MDV reactivation is unclear. As previously

521 reported for HSV-1, we can speculate that the large ribonucleotide reductase subunit

522 encoded by UL39 might contribute to the lytic switch of MDV as an auxiliary factor in the

523 viral DNA replication machinery [58]. Moreover, it was shown that UL39 mutants are

524 severely impaired for replication, establishment of latency and reactivation in murine

525 models of HSV-1 [59]. About UL49, its role in MDV reactivation under hypoxia is very

526 plausible. Indeed, we demonstrated earlier that MDV VP22 triggers DNA damages in

527 proliferating cells [51] and that induction of DNA damages with chemicals triggers MDV

528 reactivation in 3867K cells [42]. Further studies are needed to explore the role of UL49 in

529 this process, for example by mutating HREs in UL49 promoter or by ChiP assay to

530 demonstrate the binding of HIF-1 to UL49 promoter in hypoxia.

531 For some herpesviruses, caspase activities were shown to promote latent-to-lytic switch

532 and/or viral replication [38]. For example, caspase-mediated cleavage of PIAS1

533 contributes to EBV reactivation from B-cells [60]. HIF-1 being involved in the regulation of

534 apoptosis pathways [37], and a high cell death of MDV-latently infected T-cells having

535 been observed herein under hypoxia, a role of caspases in MDV reactivation was possible,

536   although never been explored before. We found that inhibition of caspase 3/7 activity

537   does not impact MDV reactivation in 3867K cultured for 48/72 h in hypoxia. This result

538   suggests that MDV reactivation triggered in hypoxia is independent of the caspase 3/7

539   activation and more likely relies on other mechanisms, discussed above.

540   Taken together, we demonstrate for the first time that hypoxia can trigger MDV

541   reactivation from transformed latently infected T-cells. With late immunodepression,

542   hypoxia is a physiological trigger of reactivation, which could explain the second lytic

543   phase observed during the Marek's disease *in vivo*. We also demonstrated that

544   overexpression of HIF1α (WT or an oxygen insensitive mutant) is sufficient to induce MDV

545   reactivation in normoxia. Thus, hypoxia and HIF-1α are new triggers of MDV reactivation.

546

547   **MATERIAL AND METHODS**

548   *Cells.*

549   Two MDV-transformed lymphoblastoid T-cell lines were used: the 3867K cell line, derived

550   from a kidney lymphoma induced by the very virulent mutant rRB-1B UL47eGFP [34] ; the

551   MSB-1 cell line, derived from a spleen lymphoma induced by a virulent strain of BC1 GaHV-2

552   strain [32, 33]. The MSB-1 has been used extensively for the analysis of MDV latency and

553   latent-to-lytic switch [61]. 3867K cells were cultured and maintained as previously described

554   [34]. MSB-1 cells were cultured in RPMI 1640 supplemented with 2 mM of glutamine and

555   10% fetal bovine serum. In normoxia, both cell lines were grown at 41°C in a standard

556   incubator in atmospheric O_2 (21% O_2 v/v), with 5% CO_2.

557   ESCDL-1 cell line used for promoter transactivation assays was cultivated as previously

558   described [62].

559

Antibodies.

561 Anti-HIF-1α (rabbit polyclonal) was obtained from Novus Biologicals (NB 100-449) and used

562 at 1:100e in immunostaining. Mouse monoclonal antibodies directed against MDV lytic

563 antigens gB (clone K11; 1:1000e), VP22 (clone B17; 1:300e) and ICP4 (clone E21; 1:1000e)

564 were previously described [63, 64] and used at dilution indicated above. As secondary

565 antibodies, goat anti-rabbit (GAR) Alexa Fluor 594 or 488 (ThermoFisher Scientific) and goat

566 anti-mouse (GAM) Alexa Fluor 555 or 594 or 488 (ThermoFisher Scientific) were used.

567

568 ***Plasmids.***

569 The pPB tdTomato, a kind gift from Bertrand Pain, is a modified PiggyBac vector (obtained

570 from Austin Smith laboratory, Cambridge, UK) expressing the tdTomato fluorescent gene

571 driven by a CAG promoter. This vector was used for measuring transfection efficiencies. The

572 pHRE-d2EGFP, a kind gift of Martin Brown and Thomas Foster, is a hypoxia reporter plasmid,

573 encoding the destabilized Enhanced Green Fluorescent Protein (EGFP) under the control of

574 hCMV minimal promoter, located downstream of five HRE from *vEGF* gene (vascular

575 Endothelial Growth Factor) (Addgene plasmid# 46926, http://n2t.net/addgene:46926 ;

576 RRID:Addgene_46926) [65]. The pHRE-d2EGFP was used as a reporter gene of HIF-1 activity.

577 The HA-HIF1α WT- pcDNA3, a kind gift from William Kaelin (Addgene plasmid # 18949 ;

578 http://n2t.net/addgene:18949 ; RRID:Addgene_18949) is a CMV promoter-driven vector

579 expressing the human wild-type (WT) form of HIF-1α [66]. The HA-HIF1α

580 P402A/P564A/N803A-pcDNA3, a kind gift from William Kaelin (Addgene plasmid # 87261 ;

581 http://n2t.net/addgene:87261 ; RRID:Addgene_87261) is a CMV promoter-driven vector

582 expressing a stabilized HIF-1α in which the three amino acids targeted by hydroxylation

583 were mutated [67]. The mutant protein is O_2 insensitive and thus resistant to proteasomal-

584   specific degradation under normoxic conditions. The HA-HIF1α WT- pcDNA3 and the HIF1α

585   P402A/P564A/N803A-pcDNA3 plasmids were used for HIF-1 α overpression in normoxia.

586

587   ***Cell culture in hypoxia.***

588   Cells were seeded at $2x10^6$ cells per mL in normoxia. One hour after division, cells were

589   placed in a hypoxia workstation (HypoxyLab, Oxford Optronix, Abingdon, UK) at 1 % O_2 v/v

590   and 5 % CO_2 (hypoxia conditions) at 41°C, and incubated during 24 to 96 h. At the time of

591   introduction in the hypoxia chamber, the cell medium contained O_2 in order to permit a

592   progressive deprivation of O_2 over the first 24 h. Due to the rapid degradation of HIF-α at

593   21% O_2, all experimental steps until cell fixation or lysis were performed within the

594   hypoxia chamber.

595

596   ***Flow cytometry analyses and cell-sorting.***

597   For 3867K cells, MDV reactivation was detected directly with UL47eGFP fluorescence by flow

598   cytometry. For live/dead analyses or live cell-sorting, cells were stained with the Fixable

599   Viability Dye eFluor 780 (ThermoFisher Scientific) according to standard procedure before

600   fixation using 1% paraformaldehyde (PFA). Flow cytometry analyses were performed either

601   with a MoFlo Astrios[EQ] flow cytometer (Beckman Coulter, Brea, USA) or with a FACS LSR

602   Fortessa cytometer (Becton Dickinson, Heidelberg, Germany). For the FACS LSR Fortessa

603   cytometer, acquisition was performed with BD FACSDiva software and analyzed with FlowJo

604   software (FlowJo LLC, Ashland, USA).

605   After Fixable Viability Dye eFluor 780 staining and 1% PFA fixation, "live cells" were sort-

606   purified by FACS gating on eFluor 780 negative with a MoFlo Astrios[EQ] flow cytometer

607   (Beckman Coulter, Brea, USA), whereas "dead cells" (eFluor 780-positive) were removed.

608

609 ***Immunostaining and fluorescence microscopy.***

610 Total cells or "live" sort-purified cells fixed in PFA were plated by centrifugation at low speed

611 (500 × g; 800rpm) for 5 min on 0.17µm-thick- glass coverslips using a Cytospin 4

612 (ThermoFisher Scientific). For MDV antigens and HIF-1α detection, the immunostainings

613 were performed for 1h in PBS, 0.1% Triton X-100, 1% bovine serum albumin (BSA). After

614 washes, the cells were incubated for 45 min with an appropriate secondary antibody(ies)

615 coupled to Alexa Fluor 488 or 555 or 594. Lastly, the nuclei were counterstained with

616 Hoechst 33342 dye (1:2000e) (Invitrogen) and the coverslips were mounted with Mowiol

617 (Merck). Such a procedure was used for cells cultivated in hypoxia, normoxia, treated with

618 pharmacological agents, as well as cells transfected with vectors expressing hHIF-1α.

619 Microscopic observations were performed using an Axiovert 200 M inverted epifluorescence

620 microscope equipped with an Apotome imaging system (Zeiss). Images were captured with

621 an AxioCam MRm charge-coupled-device camera (Zeiss) by using Axiovision software (Zeiss).

622 In several experiments, various subsets of cells were counted using Axiovision software on

623 captured images.

624

625 ***Fluorescence quantification***

626 The quantification of HIF-1 fluorescence was performed on high magnification digital

627 microscopy images using FIJI free software. First, images (HIF-1α red channel) were adjusted

628 in brightness/contrast with the Auto mode. A filter (median) was applied to all images. The

629 threshold of each image was applied with the default mode in order to visualize the cells

630 exhibiting a HIF-1α signal. The HIF-1α-positive fluorescent cells were selected with the

631 "analyze particles" tool, (small objects under 5µm were excluded). The mean grey value of

632   all selected cells was next measured (fluorescence measurement) and reported in an excel

633   table. For images, on which cells were touching each other, after the threshold setting and

634   before fluorescence measurement, cells were segmented one from the other by the "binary

635   watershed" process.

636

637   ***Sequence analysis for HREs detection in MDV complete genome.***

638   The putative HREs were identified in the MDV RB-1B complete genome (GenBank :

639   EF523390) by using a bioinformatic approach with the "dreg" tool of EMBOSS 6.6.0.0

640   software (REF:10.1016/s0168-9525(00)02024-2). The command line "dreg" was used to

641   locate in the entire genome all HREs on both strands by using the pattern "RCGTG", where

642   'R' was either an A or a G nucleotide. A local python script (available on demand) was then

643   used to compare positions of all identified HREs and positions of each known Coding DNA

644   Sequence (CDS). Thus, HREs located within a range of -700 nt and +70 nt (assuming to

645   encompass the promoter region) from the +1 of each CDS (+1 being the 'A' of the

646   transcriptional starting codon) were retained and numerated.

647

648   ***Quantification of MDV genome copy number by real‑time PCR (qPCR).***

649   DNA was extracted from 10^7 cells (3867K or MSB-1) by using QIAmp DNA mini kit according

650   to the manufacturer's instructions (Qiagen). MDV genome was quantified using TaqMan

651   technology, as previously described [27]. Briefly, for each sample, copy number of the viral

652   *ICP4* gene and the cellular *iNOS* gene were quantified independently in triplicates, in parallel

653   to standards. The positive cut-off points corresponded to 23 copies for *ICP4* and 57 copies

654   for *iNOS*. For each sample, the number of MDV genome copies are given per 10^6 cells.

655

RNA isolation and reverse transcription qPCR (RT-qPCR).

RNAs were extracted from cells (3867K or MSB-1) by using the RNeasy mini kit (#74104, Qiagen), according to the manufacturer's recommendations. RNAs were treated with RNase-free RQ1 DNase (#M6101, Promega) and RNAs concentrations were measured with a Nanodrop spectrophotometer (ThermoFisher Scientific). Five hundred ng of total RNA was reverse-transcribed by using 50µg/ml oligo(dT) primers (#C110A, Promega), dNTP (#U151A, Promega) and Moloney MLV reverse-transcriptase (#M1701, Promega). The expression of genes of interest was measured by real-time qPCR with iQ Supermix SYBR green (#1708882, Bio-Rad) in triplicate on a C1000 Touch CFX96 Real-Time PCR Detection System (Bio-Rad). The primer used for the qPCRs (viral and cellular genes) were synthetized by Eurogentec and are listed in table 2. The chicken ribosomal protein S17 gene (RPS17) was used as the reference cellular housekeeping gene. The qPCR program consisted of a 5 min activation step at 95°C, followed by 40 cycles of 95°C for 20 sec and 60°C for 35 sec. The relative changes in gene expression were calculated relatively to the expression of the RPS17 and determined by the 2^{-DDct} threshold cycle (C_T) method.

Cell treatment with pharmacological agents.

Two hypoxia-mimicking pharmacological agents were used: MLN4924, a Nedd8-Activating Enzyme Inhibitor (Pevodistat #11260, AdooQ Bioscience) and $CoCl_2$, an iron chelator which prevents hydroxylases activity and the hydroxylation of HIF α subunit (#C8661, Sigma). The stock solutions were diluted at 2.5 mM in DMSO and 50 mM in water, respectively. 3867K cells (10^6 cells/mL) were incubated with various concentrations of MLN4924 or $CoCl_2$ for 24 h. Cells were next stained for live/dead and fixed for subsequent analyses by flow cytometry analyses or fluorescence microscopy. Sodium butyrate, an inhibitor of histone deacetylases

680   was used as a positive control of reactivation. The sodium butyrate stock solution was

681   prepared at 100 mM in water and the cells treated with 0.5mM for 48 h.

682

683   ***Transient transfection and transactivation assay to monitor hHIF-1α functionality in MSB-***

684   ***1.***

685   Cells (3867K and MSB-1) were transiently transfected by using a Neon® electroporation

686   device system and the Neon transfection system 10μL kit, according to manufacturer's

687   instructions (ThermoFisher Scientific). For each transfection, $5x10^5$ cells were mixed with

688   1μg of plasmid in 10μL of re-suspension buffer. When two plasmids were co-transfected 1μg

689   of each was used. Cells were electroporated with the conditions optimized for the PB

690   tdTomato, according to manufacturer's instructions. Cells transfected with an empty plasmid

691   served as a negative control as well as mock-transfected cells (no plasmid). After

692   electroporation, the cells were seeded in 48-well plates containing 250μL of culture medium.

693   The cells were cultured for 24 h and subsequently proceeded for analysis.

694   In order to test the functionality of hHIF-1α (WT and mutant), MSB-1 were co-transfected as

695   above with a hHIF-1α vector and the pHRE-d2EGFP plasmid. The cells were then fixed,

696   plated on coverslips and counted to determine the percentage of GFP cells, as GFP

697   expression is dependent on HIF-1α functionality.

698

699   ***Caspase 3 inhibitor treatment and Caspase-Glo® 3/7 assay.***

700   3867K ($2x10^6$ cells/mL) were cultivated in hypoxia (1%) for 72 h, with or without 50μM of Z-

701   DEVD-FMK caspase 3 inhibitor (FMK004, R&D systems) in a 6-well plate. The Z-DEVD-FMK

702   stock solution was diluted in DMSO at 20mM. The Z-DEVD-FMK treatment (50μM) was

703   renewed every 24 h as well as DMSO, in the mock-treated cells. As controls, we also used

704   cells in normoxia, treated and non-treated with Z-DEVD-FMK. At 48 h and 72 h of culture,

705   luminescent caspase 3/7 activation assay was performed according to the manufacturer's

706   instructions (Caspase-Glo® 3/7 assay, Promega). Briefly, 50µl of cells treated or not (in

707   duplicate) were transferred in a white opaque 96-well plate, lysed and incubated at room

708   temperature for 1 h with Caspase-Glo® reagent. It should be noted that the cells maintained

709   in hypoxia were lysed in the hypoxia chamber, then taken out of the chamber for the room

710   temperature incubation. The luciferase activity related to the enzymatic activity of caspase-

711   3/7 was next measured using a GloMax-Multi Detection System (Promega).

712

713   ***Promoters cloning and promoter activity after HIF-1α over-expression in normoxia.***

714   The promoter regions of ICP4, ICP27, UL39, UL41, UL49 as well as UL36 and UL45 were

715   amplified by PCR from the RB-1B BAC using the Phusion Taq (NEB) and the primers depicted

716   in Table 3. UL36 and UL45 promoters lacking HRE on both DNA strands were used as MDV

717   negative control promoters. The amplified sequences were inserted into the XhoI/HindIII

718   sites upstream of a destabilized firefly luciferase gene in the pGL4.11 [*luc2P*] vector (#E666A;

719   Promega). ESCDL-1 cells were seeded on a 96-well plate ($2.5x10^4$ cells/well) 20 h before

720   transfection. Cells were co-transfected with 200ng of each pGL4.11 promoter construct and

721   10 ng of a pTK Renilla Luc (pRL). For the condition where HIF1α is overexpressed, 200ng of

722   the HA-HIF1α P402A/P564A/N803A-pcDNA3 vector was co-transfected together with the

723   reporter plasmid and pRL. Each condition was performed in quintuplicate, in two

724   independent experiments. At 24 h post-transfection, Renilla and Firefly luciferases activities

725   were measured using the dual luciferase reporter assay system (#E1910, Promega) following

726   the manufacturers' instructions and the GloMax-Multi Detection System (Promega). Firefly

727   luciferase activities were normalized with respect to Renilla luciferase activity.

Statistical analysis.

Comparison of two groups was performed by a Mann-Whitney test. Comparison of

proportions were performed by the Chi2 test or by the Fisher exact test, when the Chi2 test

was not applicable due to limited number of individuals. GraphPad prism version 7, Anastats

free softwares (https://www.anastats.fr/telechargements/) or the R software version 3.6.0

were used for plots and computing.

REFERENCES

1. Roizman B (2013) Herpesviridae. In: Knipe D.M., Howley P.M. (eds.) Fields Virology. Lippincott Williams & Wilkins, Philadelphia, pp. 1802-1822
2. Roizman B, Whitley RJ (2013) An inquiry into the molecular basis of HSV latency and reactivation. Annu Rev Microbiol 67:355-374
3. Stowe RP, Kozlova EV, Yetman DL, Walling DM, Goodwin JS, Glaser R (2007) Chronic herpesvirus reactivation occurs in aging. Exp Gerontol 42:563-570
4. Davis DA, Rinderknecht AS, Zoeteweij JP, Aoki Y, Read-Connole EL, Tosato G, Blauvelt A, Yarchoan R (2001) Hypoxia induces lytic replication of Kaposi sarcoma-associated herpesvirus. Blood 97:3244-3250
5. Jiang JH, Wang N, Li A, Liao WT, Pan ZG, Mai SJ, Li DJ, Zeng MS, Wen JM, Zeng YX (2006) Hypoxia can contribute to the induction of the Epstein-Barr virus (EBV) lytic cycle. J Clin Virol 37:98-103

757 6.   Polcicova K, Hrabovska Z, Mistrikova J, Tomaskova J, Pastorek J, Pastorekova S,
758   Kopacek J (2008) Up-regulation of Murid herpesvirus 4 ORF50 by hypoxia: possible
759   implication for virus reactivation from latency. Virus Res 132:257-262
760 7.   Kraus RJ, Yu X, Cordes BA, Sathiamoorthi S, Iempridee T, Nawandar DM, Ma S,
761   Romero-Masters JC, McChesney KG, Lin Z, Makielski KR, Lee DL, Lambert PF,
762   Johannsen EC, Kenney SC, Mertz JE (2017) Hypoxia-inducible factor-1alpha plays
763   roles in Epstein-Barr virus's natural life cycle and tumorigenesis by inducing lytic
764   infection through direct binding to the immediate-early BZLF1 gene promoter. PLoS
765   Pathog 13:e1006404
766 8.   Haque M, Davis DA, Wang V, Widmer I, Yarchoan R (2003) Kaposi's sarcoma-
767   associated herpesvirus (human herpesvirus 8) contains hypoxia response elements:
768   relevance to lytic induction by hypoxia. J Virol 77:6761-6768
769 9.   Cai Q, Lan K, Verma SC, Si H, Lin D, Robertson ES (2006) Kaposi's sarcoma-associated
770   herpesvirus latent protein LANA interacts with HIF-1 alpha to upregulate RTA
771   expression during hypoxia: Latency control under low oxygen conditions. J Virol
772   80:7965-7975
773 10. Semenza GL (2003) Targeting HIF-1 for cancer therapy. Nat Rev Cancer 3:721-732
774 11. Loenarz C, Coleman ML, Boleininger A, Schierwater B, Holland PW, Ratcliffe PJ,
775   Schofield CJ (2011) The hypoxia-inducible transcription factor pathway regulates
776   oxygen sensing in the simplest animal, Trichoplax adhaerens. EMBO Rep 12:63-70
777 12. Brahimi-Horn MC, Pouyssegur J (2009) HIF at a glance. J Cell Sci 122:1055-1057
778 13. Huang LE, Gu J, Schau M, Bunn HF (1998) Regulation of hypoxia-inducible factor
779   1alpha is mediated by an O2-dependent degradation domain via the ubiquitin-
780   proteasome pathway. Proc Natl Acad Sci U S A 95:7987-7992
781 14. Bruick RK, McKnight SL (2001) A conserved family of prolyl-4-hydroxylases that
782   modify HIF. Science 294:1337-1340
783 15. Kaelin WG, Jr., Ratcliffe PJ (2008) Oxygen sensing by metazoans: the central role of
784   the HIF hydroxylase pathway. Mol Cell 30:393-402
785 16. Calnek BW (1998) Lymphomagenesis in Marek's Disease. Avian Pathol 27:S54-S64
786 17. Schat KA, Nair V (2008) Marek's Disease. In: Saif Y.M. (ed) Disease of Poultry.
787   Blackwell Publishing Ltd, Ames, pp. 452-514
788 18. Calnek BW (1986) Marek's disease--a model for herpesvirus oncology. Crit Rev
789   Microbiol 12:293-320
790 19. Delecluse HJ, Hammerschmidt W (1993) Status of Marek's disease virus in
791   established lymphoma cell lines: herpesvirus integration is common. J Virol 67:82-92
792 20. Kaufer BB, Jarosinski KW, Osterrieder N (2011) Herpesvirus telomeric repeats
793   facilitate genomic integration into host telomeres and mobilization of viral DNA
794   during reactivation. J Exp Med 208:605-615
795 21. Osterrieder N, Wallaschek N, Kaufer BB (2014) Herpesvirus Genome Integration into
796   Telomeric Repeats of Host Cell Chromosomes. Annu Rev Virol 1:215-235
797 22. Jones D, Lee L, Liu JL, Kung HJ, Tillotson JK (1992) Marek disease virus encodes a
798   basic-leucine zipper gene resembling the fos/jun oncogenes that is highly expressed
799   in lymphoblastoid tumors. Proc Natl Acad Sci U S A 89:4042-4046
800 23. Cantello JL, Anderson AS, Morgan RW (1994) Identification of latency-associated
801   transcripts that map antisense to the ICP4 homolog gene of Marek's disease virus. J
802   Virol 68:6280-6290

803   24.   Cantello JL, Parcells MS, Anderson AS, Morgan RW (1997) Marek's disease virus
804   latency-associated transcripts belong to a family of spliced RNAs that are antisense to
805   the ICP4 homolog gene. J Virol 71:1353-1361
806   25.   Burnside J, Bernberg E, Anderson A, Lu C, Meyers BC, Green PJ, Jain N, Isaacs G,
807   Morgan RW (2006) Marek's disease virus encodes MicroRNAs that map to meq and
808   the latency-associated transcript. J Virol 80:8778-8786
809   26.   Yao Y, Zhao Y, Xu H, Smith LP, Lawrie CH, Watson M, Nair V (2008) MicroRNA profile
810   of Marek's disease virus-transformed T-cell line MSB-1: predominance of virus-
811   encoded microRNAs. J Virol 82:4007-4015
812   27.   Rémy S, Blondeau C, Le Vern Y, Lemesle M, Vautherot J-F, Denesvre C (2013)
813   Fluorescent tagging of VP22 in N-terminus reveals that VP22 favors Marek's disease
814   virus virulence in chickens and allows morphogenesis study in MD tumor cells. Vet
815   Res 44:125
816   28.   Parcells MS, Arumugaswami V, Prigge JT, Pandya K, Dienglewicz RL (2003) Marek's
817   disease virus reactivation from latency: changes in gene expression at the origin of
818   replication. Poult Sci 82:893-898
819   29.   Fleming IN, Manavaki R, Blower PJ, West C, Williams KJ, Harris AL, Domarkas J, Lord S,
820   Baldry C, Gilbert FJ (2015) Imaging tumour hypoxia with positron emission
821   tomography. Br J Cancer 112:238-250
822   30.   Vaupel P, Kallinowski F, Okunieff P (1989) Blood flow, oxygen and nutrient supply,
823   and metabolic microenvironment of human tumors: a review. Cancer Res 49:6449-
824   6465
825   31.   Bertout JA, Patel SA, Simon MC (2008) The impact of O2 availability on human
826   cancer. Nat Rev Cancer 8:967-975
827   32.   Akiyama Y, Kato A (1973) Continuous cell culture from lymphoma of Marek's disease.
828   Biken Journal 16:177-179
829   33.   Akiyama Y, Kato S (1974) Two cell lines from lymphomas of Marek's disease. Biken J
830   17:105-116
831   34.   Denesvre C, Rémy S, Fragnet L, Smith LP, Georgeault S, Vautherot J-F, Nair V (2016)
832   Marek's disease virus undergoes complete morphogenesis after reactivation in T-
833   lymphoblastoid cell line transformed by recombinant fluorescent marker virus. J.
834   Gen. Virol. 97:480-486
835   35.   Jarosinski KW, Arndt S, Kaufer BB, Osterrieder N (2012) Fluorescently tagged pUL47
836   of Marek's disease virus reveals differential tissue expression of the tegument
837   protein in vivo. J Virol 86:2428-2436
838   36.   Spatz SJ, Zhao Y, Petherbridge L, Smith LP, Baigent SJ, Nair V (2007) Comparative
839   sequence analysis of a highly oncogenic but horizontal spread-defective clone of
840   Marek's disease virus. Virus Genes 35:753-766
841   37.   Greijer AE, van der Wall E (2004) The role of hypoxia inducible factor 1 (HIF-1) in
842   hypoxia induced apoptosis. J Clin Pathol 57:1009-1014
843   38.   Tabtieng T, Gaglia MM (2018) Emerging Proviral Roles of Caspases during Lytic
844   Replication of Gammaherpesviruses. J Virol 92
845   39.   Lieberman PM (2016) Epigenetics and Genetics of Viral Latency. Cell Host Microbe
846   19:619-628
847   40.   Brown AC, Nair V, Allday MJ (2012) Epigenetic regulation of the latency-associated
848   region of Marek's disease virus in tumor-derived T-cell lines and primary lymphoma. J
849   Virol 86:1683-1695

850   41.   Parcells MS, Dienglewicz RL, Anderson AS, Morgan RW (1999) Recombinant Marek's
851   disease virus (MDV)-derived lymphoblastoid cell lines: regulation of a marker gene
852   within the context of the MDV genome. J Virol 73:1362-1373
853   42.   Bencherit D, Rémy S, Le Vern Y, Vychodil T, Bertzbach LD, Kaufer BB, Denesvre C,
854   Trapp-Fragnet L (2017) Induction of DNA damages upon Marek's disease virus
855   infection: implication in viral replication and pathogenesis. J. Virol. 91:1-36
856   43.   Postema EJ, McEwan AJ, Riauka TA, Kumar P, Richmond DA, Abrams DN, Wiebe LI
857   (2009) Initial results of hypoxia imaging using 1-alpha-D: -(5-deoxy-5-[18F]-
858   fluoroarabinofuranosyl)-2-nitroimidazole (18F-FAZA). Eur J Nucl Med Mol Imaging
859   36:1565-1573
860   44.   Sendoel A, Hengartner MO (2014) Apoptotic cell death under hypoxia. Physiology
861   (Bethesda) 29:168-176
862   45.   Chiche J, Rouleau M, Gounon P, Brahimi-Horn MC, Pouyssegur J, Mazure NM (2010)
863   Hypoxic enlarged mitochondria protect cancer cells from apoptotic stimuli. J Cell
864   Physiol 222:648-657
865   46.   Sasabe E, Tatemoto Y, Li D, Yamamoto T, Osaki T (2005) Mechanism of HIF-1alpha-
866   dependent suppression of hypoxia-induced apoptosis in squamous cell carcinoma
867   cells. Cancer Sci 96:394-402
868   47.   Schmaltz C, Hardenbergh PH, Wells A, Fisher DE (1998) Regulation of proliferation-
869   survival decisions during tumor cell hypoxia. Mol Cell Biol 18:2845-2854
870   48.   Tafani M, Sansone L, Limana F, Arcangeli T, De Santis E, Polese M, Fini M, Russo MA
871   (2016) The Interplay of Reactive Oxygen Species, Hypoxia, Inflammation, and Sirtuins
872   in Cancer Initiation and Progression. Oxid Med Cell Longev 2016:3907147
873   49.   Redza-Dutordoir M, Averill-Bates DA (2016) Activation of apoptosis signalling
874   pathways by reactive oxygen species. Biochim Biophys Acta 1863:2977-2992
875   50.   Carmeliet P, Dor Y, Herbert JM, Fukumura D, Brusselmans K, Dewerchin M, Neeman
876   M, Bono F, Abramovitch R, Maxwell P, Koch CJ, Ratcliffe P, Moons L, Jain RK, Collen D,
877   Keshert E (1998) Role of HIF-1alpha in hypoxia-mediated apoptosis, cell proliferation
878   and tumour angiogenesis. Nature 394:485-490
879   51.   Trapp-Fragnet L, Bencherit D, Chabanne-Vautherot D, Le Vern Y, Rémy S, Boutet-
880   Robinet E, Mirey G, Vautherot JF, Denesvre C (2014) Cell cycle modulation by Marek's
881   disease virus: the tegument protein VP22 triggers S-phase arrest and DNA damage in
882   proliferating cells. PLoS One 9:e100004
883   52.   Kallio PJ, Okamoto K, O'Brien S, Carrero P, Makino Y, Tanaka H, Poellinger L (1998)
884   Signal transduction in hypoxic cells: inducible nuclear translocation and recruitment
885   of the CBP/p300 coactivator by the hypoxia-inducible factor-1alpha. EMBO J 17:6573-
886   6586
887   53.   Soucy TA, Smith PG, Milhollen MA, Berger AJ, Gavin JM, Adhikari S, Brownell JE,
888   Burke KE, Cardin DP, Critchley S, Cullis CA, Doucette A, Garnsey JJ, Gaulin JL,
889   Gershman RE, Lublinsky AR, McDonald A, Mizutani H, Narayanan U, Olhava EJ, Peluso
890   S, Rezaei M, Sintchak MD, Talreja T, Thomas MP, Traore T, Vyskocil S, Weatherhead
891   GS, Yu J, Zhang J, Dick LR, Claiborne CF, Rolfe M, Bolen JB, Langston SP (2009) An
892   inhibitor of NEDD8-activating enzyme as a new approach to treat cancer. Nature
893   458:732-736
894   54.   Brown JS, Jackson SP (2015) Ubiquitylation, neddylation and the DNA damage
895   response. Open Biol 5:150018

896   55.   Takahashi T, Sugishita Y, Nojiri T, Shimizu T, Yao A, Kinugawa K, Harada K, Nagai R
897   (2001) Cloning of hypoxia-inducible factor 1alpha cDNA from chick embryonic
898   ventricular myocytes. Biochem Biophys Res Commun 281:1057-1062

899   56.   Mole DR, Blancher C, Copley RR, Pollard PJ, Gleadle JM, Ragoussis J, Ratcliffe PJ
900   (2009) Genome-wide association of hypoxia-inducible factor (HIF)-1alpha and HIF-
901   2alpha DNA binding with expression profiling of hypoxia-inducible transcripts. J Biol
902   Chem 284:16767-16775

903   57.   Choudhry H, Harris AL (2018) Advances in Hypoxia-Inducible Factor Biology. Cell
904   Metab 27:281-298

905   58.   Packard JE, Dembowski JA (2021) HSV-1 DNA Replication-Coordinated Regulation by
906   Viral and Cellular Factors. Viruses 13

907   59.   Mostafa HH, Thompson TW, Konen AJ, Haenchen SD, Hilliard JG, Macdonald SJ,
908   Morrison LA, Davido DJ (2018) Herpes Simplex Virus 1 Mutant with Point Mutations
909   in UL39 Is Impaired for Acute Viral Replication in Mice, Establishment of Latency, and
910   Explant-Induced Reactivation. J Virol 92

911   60.   Zhang K, Lv DW, Li R (2017) B Cell Receptor Activation and Chemical Induction Trigger
912   Caspase-Mediated Cleavage of PIAS1 to Facilitate Epstein-Barr Virus Reactivation.
913   Cell Rep 21:3445-3457

914   61.   Morgan RW, Xie Q, Cantello JL, Miles AM, Bernberg EL, Kent J, Anderson A (2001)
915   Marek's disease virus latency. Curr Top Microbiol Immunol 255:223-243

916   62.   Vautherot JF, Jean C, Fragnet-Trapp L, Remy S, Chabanne-Vautherot D, Montillet G,
917   Fuet A, Denesvre C, Pain B (2017) ESCDL-1, a new cell line derived from chicken
918   embryonic stem cells, supports efficient replication of Mardiviruses. PLoS One
919   12:e0175259

920   63.   Dorange F, El Mehdaoui S, Pichon C, Coursaget P, Vautherot JF (2000) Marek's
921   disease virus (MDV) homologues of herpes simplex virus type 1 UL49 (VP22) and
922   UL48 (VP16) genes: high-level expression and characterization of MDV-1 VP22 and
923   VP16. J Gen Virol 81:2219-2230.

924   64.   Blondeau C, Chbab N, Beaumont C, Courvoisier K, Osterrieder N, Vautherot J-F,
925   Denesvre C (2007) A full UL13 open reading frame in Marek's disease virus (MDV) is
926   dispensable for tumor formation and feather follicle tropism and cannot restore
927   horizontal virus transmission of rRB-1B in vivo. Vet Res 38:419-433

928   65.   Vordermark D, Shibata T, Brown JM (2001) Green fluorescent protein is a suitable
929   reporter of tumor hypoxia despite an oxygen requirement for chromophore
930   formation. Neoplasia 3:527-534

931   66.   Kondo K, Klco J, Nakamura E, Lechpammer M, Kaelin WG, Jr. (2002) Inhibition of HIF
932   is necessary for tumor suppression by the von Hippel-Lindau protein. Cancer Cell
933   1:237-246

934   67.   Yan Q, Bartz S, Mao M, Li L, Kaelin WG, Jr. (2007) The hypoxia-inducible factor 2alpha
935   N-terminal and C-terminal transactivation domains cooperate to promote renal
936   tumorigenesis in vivo. Mol Cell Biol 27:2092-2102

937

938

FIGURE LEGENDS

940 **Figure 1. Hypoxia induces MDV reactivation in 3867K, a T-cell line latently infected with**

941 **RB-1B UL47eGFP**. (A) Viral reactivation and mortality. 3867K cells were cultivated for 72 h in

942 normoxia or hypoxia (1% O_2). Viral reactivation and mortality were analyzed by flow

943 cytometry. Reactivation was measured directly through the UL47eGFP signal, a protein

944 expressed in lytic cycle, whereas mortality was visualized with the fixable viability dye

945 eFluor780. The percentage of cells in lytic cycle and of dead cells (eFluor780-positive) is

946 given in hypoxia and normoxia relatively to the total cell number. The mean of green

947 fluorescence for latently-infected cells and cells in lytic cycle is also shown in green on the

948 bottom of both diagrams in arbitrary unit. (B) Images of 3867K cultivated in normoxia and

949 hypoxia for 72 h observed by fluorescence microscopy. The cells were stained with an

950 antibody recognizing VP22 or gB lytic proteins (red), in addition to UL47eGFP (green) and

951 Hoechst 33342 for DNA (blue). Bar, 20μm. (C) Two cell populations (live/green; dead/green)

952 were sorted by flow cytometry after 48 h in hypoxia and normoxia. Cells were labeled with

953 an antibody directed against the VP22 lytic protein and observed by fluorescence

954 microscopy. The VP22 signal (Red) was clearly visible in some live green cells, but never in

955 dead green cells. Bar, 20μm. (D) Kinetic of viral reactivation upon cultivation in hypoxia.

956 3867K were cultivated in normoxia (Nx, dashes grey line) and hypoxia (Hx, plain black line)

957 for 96 h and the viral reactivation measured every 24 h based on UL47eGFP signal by flow

958 cytometry. The % of GFP-positive cells was calculated among live cells. The graph is the

959 result of two independent experiments, with each dot of the curve being the median. (E) The

960 MDV genome copy number upon hypoxia cultivation. 3867K were cultivated in normoxia

961 (Nx, dashes grey line) and hypoxia (Hx, plain black line) for 96 h and the genome copy

number per million cells was measured every 24 h by absolute qPCR. The graph is the result

of two independent experiments, with each dot of the curve corresponding to the median.

Figure 2. **MDV lytic genes expression is upregulated during hypoxia.** (A) Schematic diagram

of RB-1B genome (Genbank #EF523390) with 16 selected lytic genes. The number of putative

HREs identified in the promoter region is given in brackets after each gene name. (B) Heat

map showing the differential genes expression of 16 lytic genes as well a *meq* oncogene

upon cultivation in hypoxia relatively to normoxia over 72 h. The gene expression was

quantified every 24 h and the results are given in fold-changes (scale with colors on the

right). This heat-map is representative of two independent experiments.

Figure 3. Hypoxia induces MDV reactivation in MSB-1, a T-cell line latently infected with

the BC-1 strain. (A) Viral reactivation assessed by genome copy number measurement. MSB-

1 cells were cultivated in normoxia (Nx, dashes grey line) and hypoxia (Hx, plain black line)

for 96 h and the genome copy number per million cells was measured every 24 h by absolute

qPCR. (B) Images of MSB-1 cultivated in normoxia and hypoxia for 24 and 48 h observed by

fluorescence microscopy. The cells were stained with an antibody recognizing the VP22 lytic

protein (red) and with Hoechst 33342 for nuclei (blue). Bar, 20 μm. The % of reactivation

determined by counting the VP22-positive cells relatively to the cells harboring a non-

fragmented nucleus (given as n) is shown on each picture. (C) Heat map showing the

differential genes expression of 16 lytic genes as well a *meq* oncogene upon MSB-1

cultivation in hypoxia relatively to normoxia at three time points (24, 48 and 72 h). The

results are given in fold-changes (scale with colors on the right).

986 **Figure 4. Hypoxia induces MDV reactivation in a subset of HIF-1α-positive cells.** 3867K (A)

987 and MSB-1 (B) were cultivated in normoxia and hypoxia for 48 h. After fixation, "live cells"

988 (eFluor780-negative) were cell-sorted by flow cytometry, stained with an antibody

989 recognizing HIF-1α (in red) and Hoechst 33342 for DNA (blue). (A) For 3867K, reactivation

990 was detected directly with UL47eGFP (green). (B) For MSB-1, reactivation was detected after

991 staining with an antibody against the lytic VP22 protein (green). For each cell line, single

992 channel and overlay images are shown. Bar, 20μm. 3867K and MSB-1 showed a low HIF-1α

993 signal in hypoxia and not in normoxia. A small subset of HIF-1α-positive cells were in

994 reactivation. The fluorescence intensity of HIF-1α per cell was quantified in normoxia and

995 hypoxia in 3867K (C) and MSB-1 (D) cells.

996

997 **Figure 5. Hypoxia enhances expression of HIF-1-responsive cellular genes in MDV latently**

998 **infected-T cells**. 3867K (A) and MSB-1 (B) cells were cultivated in normoxia or in hypoxia for

999 72 or 96 h. The mRNA levels of three HIF-1 regulated cellular genes were quantified by RT-

1000 qPCR every 24 h and normalized to the RPS-17 gene. mRNA levels are expressed as fold-

1001 change in hypoxia relative to normoxia, from one (MSB-1) or two (3867K) independent

1002 experiments. The dots correspond to the fold-change of two independent samples, with

1003 three technical qPCR repeats each. The median is shown as a long horizontal bar.

1004

1005 **Figure 6. HIF1α stabilizers induce MDV reactivation in normoxia in MDV latently infected-T**

1006 **cells**. 3867K cultivated in normoxia were treated with different concentrations of CoCl2 or

1007 MLN4924 for 24 h. A. Percentage of reactivation (GFP-positive cells) measured on live cells

1008 on two independent experiments. After each treatment, cells were stained with the fixable

1009 viability dye eFluor780 and analyzed by flow cytometry, for GFP and eFluor780 fluorescence.

1010 The fold changes were calculated relatively to mock-treated cells (Ctrl) (water for CoCl2 and

1011 DMSO for MLN4924). A positive reactivation control was performed with 0.5mM sodium

1012 butyrate (NaBu) for 48 h (n=3 for each condition). B. Expression of HIF-1α and MDV antigens

1013 in 3867K treated with 1µM MLN4924 for 24 h observed by fluorescent microscopy. After

1014 treatment, cells were fixed, centrifuged at low speed on coverslips and stained with

1015 VP22/ICP4 antibodies cocktail (green), HIF-1α antibody (red) and Hoechst 33342 for DNA

1016 (blue). Bar, 20µm. C. The mRNA levels of four viral lytic genes and two HIF-1 regulated

1017 cellular genes were quantified by RT-qPCR after 1µM MLN4924 treatment for 24 h. mRNA

1018 levels are expressed as fold-change relative to RPS-17, from two independent experiments

1019 (with technical triplicates). Each dot corresponds to a single measure. The median is shown

1020 as a long horizontal bar.

1021

1022 **Figure 7. Human HIF-1α is functional in chicken T-cells**. hHIF-1α activity was monitored with

1023 a transactivation assay in normoxia. MSB-1 were transiently co-transfected with pHRE-

1024 d2EGFP reporter plasmid with or without a pCDNA vector expressing HIF-1α, either the

1025 stabilized mutant (P402A/P564A/N803A) (A) or the WT (B). The % of GFP cells was

1026 enumerated by fluorescence microscopy. At least 900 cells were counted in each condition.

1027 For each condition, an image of the cells at 24 h post-transfection is shown. The difference in

1028 GFP-positive cells proportion was significant at each time post-transfection, for both HIF-1

1029 (WT and mutant) (p-value <0.0001, ***; Chi2 test). Bar, 20µm.

1030

1031 **Figure 8. HIF-1α overexpression induces MDV reactivation in MSB-1 in normoxia.** MSB-1

1032 were transfected with the pCDNA vector expressing hHIF-1α mutant or WT, an empty

1033 pCDNA vector or mock-transfected. At 24 h post-transfection, the cells were fixed,

1034   centrifuged at low speed on coverslips, and stained with MDV antigens (VP22/ICP4)

1035   antibodies cocktail (green), HIF-1α antibody (red) and Hoechst 33342 for DNA (blue). (A) The

1036   percentage of HIF-1α-positive cells in each condition. The difference in HIF-1α-positive cells

1037   proportion was significant between WT and mutant and between mutant and pcDNA3

1038   control (adjusted p-value <0.0001, ***; Fisher exact test with a Holm correction for multiple

1039   comparison). (B) The percentage of reactivated cells based on MDV antigens-positive cells in

1040   each condition. The difference in EGFP-positive cells proportion was significant when HIF-1α

1041   (WT or mutant) was present vs pcDNA3 (adjusted p-value <0.0001, ***; Fisher exact test

1042   with a Holm correction for multiple comparison). (C) The percentage of HIF-1α-positive cells

1043   which were also MDV antigens-positive (reactivated) in each condition. The differences were

1044   not significant (adjusted p-value >0.05; Fisher exact test with a Holm correction for multiple

1045   comparison) (D). Images of MSB-1 transfected with HIF-1α mut or WT, which were

1046   reactivated and HIF-1α positive (green and red; left panel) as well as reactivated and HIF-1α

1047   negative (green only; right panel). Bar, 20µm.

1048

1049   **Figure 9. HIF-1α over-expression activates MDV UL39 and UL49 promoters**. A. The

1050   expression of hHIF-1α was validated in ESCDL-1, after transient transfection with the hHIFα

1051   mut expression vector. The hHIF-1α (red) was detected by fluorescence microscopy as

1052   previously. Two cells showed a strong nuclear expression. B. ESCDL-1 cells were co-

1053   transfected with a MDV promoter cloned in 5' of a destabilized fLuc gene in pGL4 vector, a

1054   TK renilla luciferase (RL) vector for transfection efficacy normalization, with or without the

1055   hHIFα mut expression vector. The promoters from seven MDV genes were tested, 5 with

1056   HRE (ICP4, ICP27, UL39, UL41 and UL49) and 2 without HRE (UL36, UL45). An empty pGL4

1057   was also assayed as control. Twenty-four hours post-transfection the fluc and RL activities

1058   were measured and the fLuc activity normalized with the RL activity. Each circle represents

1059   independent transfection, with hHIF-1α (black circle) or without hHIF-1α (white circle). The

1060   horizontal bars represent the median of the quintuplicate. This experiment is representative

1061   of at least 2 independent experiments. The differences were significant between with and

1062   without hHIFα mut (Mann-Whitney test, p-value <0.01, **). UL39 and UL49 promoters had a

1063   strong relative luciferase activity in presence of hHIFα mut, compared to the other

1064   promoters tested (with or without HRE).

1065

1066   **Figure 10**. **Apoptosis mediated by caspase 3 in hypoxia is not promoting MDV reactivation.**

1067   A. 3867K cultivated in normoxia were treated or not with 50µM of Z-DEVD-FMK for 24 h, and

1068   the caspase 3/7 activity was next measured with the luminescent Caspase 3/7-Glo® assay.

1069   The difference was significant between cells treated and non-treated with Z-DEVD-FMK

1070   (Mann-Whitney test, p-value =0.0022, **). B. 3867K were cultivated in hypoxia with or

1071   without 50µM of Z-DEVD-FMK. The caspase 3/7 activity (black dots, replicates from two

1072   independent experiments) was measured at 48 h and 72 h. At both timepoints, the

1073   differences were significant (Mann-Whitney test, p-value <0.01, **). In parallel, the

1074   percentage of reactivated cells among live cells (green squares) from two independent

1075   experiments was measured based on UL47eGFP signal and cell mortality quantified by flow

1076   cytometry.

1077

1078

1079 **Table 1.** Percentage of dead cells in 3867K and MSB-1 during hypoxia or normoxia
1080 cultivation

1081

	24 h		48 h		7 2h		96 h	
	Normoxia	**Hypoxia**	**Normoxia**	**Hypoxia**	**Normoxia**	**Hypoxia**	**Normoxia**	**Hypoxia**
3867K Expt#1	20.63	32.35	13.15	44.11	12.52	51.79	14.35	52.36
Expt#2	21.93	39.92	19.00	48.66	20.99	59.34	25.22	66.42
MSB-1	25.85	57.96	28.80	79.22	34.10	85.07	44.31	85.61

1082

1083

1084

Table 2. Viral and cellular primers used in this study for RT-qPCR

Gene name	Forward primer sequence (5' to 3')	Reverse primer sequence (5' to 3')	NCBI Reference sequence
MDV			EF523390
ICP4	TTTCTAGCAAGGAGCGACGC	CGTACTTGCGCTTACGGGAA	
ICP27	CTCGCGAGTCCGATGACATG	GTTCCTGCGTACACGGTGGC	
UL39	ACGGGGGTAGCAAATTGGAG	CAGCTCGCAGTAGAGGTTCC	
UL42	TTAGCGACGACGGACTGATG	CCCGCGCCATTCATATTCAC	
UL30	CTGTTGGGGACACTATGCGT	CCGATTCCGCTTCGTATCGT	
UL41	CCCGGGGTGTTTCCTCTTAC	TTCTGGGCGACTACATGCAC	
pp38	TTGCATTCTCTGACTCCACGG	GCTGGCCGAAAGACAAAACC	
UL31	GCTCTGTCGTTTCGTCCCAA	GAGGCGGTTGCGGATAACT	
UL34	CGATGAAACGCACAGAAGTGG	ATCGTCGTCACACATTCGCC	
UL13	GGGATTAGGACCCTCGGTGA	TCTCGGCAAAGCAGTTGTGT	
UL47	GTATCACTACCGCGACGACC	CGATACGCTAGAGGAGAGCG	
UL48	CAGGAGCAGTCAAAACACGC	CTTTCTACCACGCGGGATGT	
UL49-VP22	TGCTCGCAGACCATCAACAC	GAAACGTCTTCCGATACGGC	
UL27-gB	GTCCGATAGAACGGCGGTAG	TGAGTTGCATGGCGAGGAAT	
UL44-gC	GCCGCATTCCAGTATGGGAC	CTTCATCGAAGGGGTAGCC	
US7-gI	CCTCTTTCGAGGCATCTGGT	AATCCGCAGAACGCAACAAG	
meq	GTCCCCCTCGATCTTTCTC	CGTCTGCTTCCTGCGTCTTC	
Gallus gallus			
GLUT1	GAGAGCGGCAGCAAGATGAC	CTTCTGCGGGCGATTGATGA	NM_205209
LDHA	TTAACTTGGCCAACGCAACGTCAAT	TCCACTGGGTTTGAGACAATCAG	NM_205284
iNOS	TACTGCGTGTCCTTTCAACG	CCCATTCTTCTTCCAACCTC	NM_204961
RPS17	ACACCCGTCTGGGCAACGAC	CCCGCTGGATGCGCTTCATC	NM_204217

Table 3. Primers used in this study for MDV promoters cloning

Gene name	Primer sequence (5' to 3')*	Amplicon length (bp)
UL39XhoI	GTC**CTCGAG**CTTCATCATCTCTATACCTTGTG	712
UL39HindIII	CTG**AAGCTT**AGCAGATTTTTAGTCGCAGAGTG	
UL41XhoI	CTG**CTCGAG**ATAATTGCAATGCGCATGTTCTA	512
UL41HindIII	CTG**AAGCTT**GATGACCCTCGCAGTTTTTAAATAT	
UL49XhoI	CTG**CTCGAG**ATTGCAGACGCCAGGGAACTGTT	512
UL49HindIII	CTG**AAGCTT**GATAACTAAGATATAATATTAAA	
ICP4XhoI	CTG**CTCGAG**CCTGATACCGCACTTTG	452
ICP4HindIII	CTG**AAGCTT**AATCCCCACGTCTTCGTCAAAAGC	
ICP27XhoI	CTG**CTCGAG**CTATCGATGTATTTTGTACCATG	536
ICP27HindIII	CTG**AAGCTT**GCGAGAGAATGCATCTACAGACA	
UL36XhoI	CTG**CTCGAG**CGGTGAAATAGAATTTGCCG	512
UL36HindIII	CTG**AAGCTT**TTTACACTCAATTTATATGA	
UL45XhoI	CTG**CTCGAG**TTTGTCATGGAGATATCGTC	512
UL45HindIII	CTG**AAGCTT**TCTTATACGATCATGTCTAT	

1089   * restriction sites in bold
1090

Figure 1

A

Normoxia

eFluor780

3.9   37.3
      12.52 %
      0.85%
5.1   73.6

GFP

Hypoxia

eFluor780

9.8   42.1
      51.79 %
      4.03%
9.4   67.5

GFP

B

UL47eGFP & VP22 (red)

Normoxia

Hypoxia

UL47eGFP & gB (red)

Normoxia

Hypoxia

C

Green fluorescent-positive cells

eFluor-   eFluor+

Normoxia

Hypoxia

DNA/ green fluorescence/ VP22

D

% of viral reactivation among live cells

10

5

0

24   48   72   96

Time (h)

Hx

Nx

E

MDV Genome copy number per 10⁶ cells

3×10⁸

2×10⁸

1×10⁸

24   48   72   96

Time (h)

Hx

Nx

Figure 2

A

Lytic genes

Immediate Early
Early
Late

(Number of putative HRE in the promotor)

UL13 (0) UL27 (0) UL31 (1) UL41 (2) UL47 (1) UL48 (0) UL49 (3) pp38 (3) ICP4 (1)

pp24 (3) UL30 (1) UL34 (2) UL39 (2) UL42 (3) UL44 (3) ICP27 (1) US7 (3) ICP4 (1)

TR_L   UL   IR_L   IR_S   US   TR_S

B

3867K cells

		24 h	48 h	72 h
IE	ICP4	18	20	56
	ICP27	16	25	47
E	UL39 – RR1	28	18	42
	UL42	5	18	28
	UL30	8	17	11
	UL41 – VHS	12	25	48
	pp38	4	13	14
L	UL31	4	14	19
	UL34	4	13	15
	UL13	3	16	19
	UL48 – VP16	4	13	16
	UL49 – VP22	17	24	44
	UL47	4	16	18
	UL27 – gB	4	14	11
	UL44 – gC	3	11	12
	US7 – gI	7	31	60
	Meq	5	4	8

Figure 3

A

B

	24 h	48 h
Normoxia	**0.96%** VP22+ (n=2806)	**0.84%** VP22+ (n=1780)
Hypoxia	**3.16%** VP22+ (n=1331)	**7.30%** VP22+ (n=795)

VP22 ; Hoechst 33342

C

MSB-1 cells

		24 h	48 h	72 h
IE	ICP4	4	35	31
	ICP27	5	24	20
E	UL39 – RR1	15	74	26
	UL42	3	14	13
	UL30	5	19	9
	UL41 – VHS	3	54	17
	pp38	2	15	9
L	UL31	5	23	17
	UL34	4	20	17
	UL13	2	11	22
	UL48 – VP16	5	19	6
	UL49 – VP22	13	68	25
	UL47	4	54	18
	UL27 – gB	5	17	5
	UL44 – gC	3	21	6
	US7 – gI	3	38	40
	Meq	1	3	3

Figure 4

Figure 5

A 3867K

B MSB-1

Figure 6

Figure 7

A

Stabilized HIF-1α mutant

n = 1221 n = 971 n = 1186 n = 976 n = 3300 n = 1496

**** **** ****

% of GFP cells

30

20

10

0

Time post-transfection (h)

8   24   48

■ pHRE-d2EGFP
■ pHRE-d2EGFP + hHIF-1α mutant

B

HIF-1α WT

n = 1634 n = 857 n = 1389 n = 1482 n = 1340 n = 605

**** **** ****

% of GFP cells

30

20

10

0

Time post-transfection (h)

8   24   48

■ pHRE-d2EGFP
■ pHRE-d2EGFP + hHIF-1α WT

24 h post-transfection

None   HIF-1α mutant

24 h post-transfection

None   HIF-1α WT

Figure 8

A
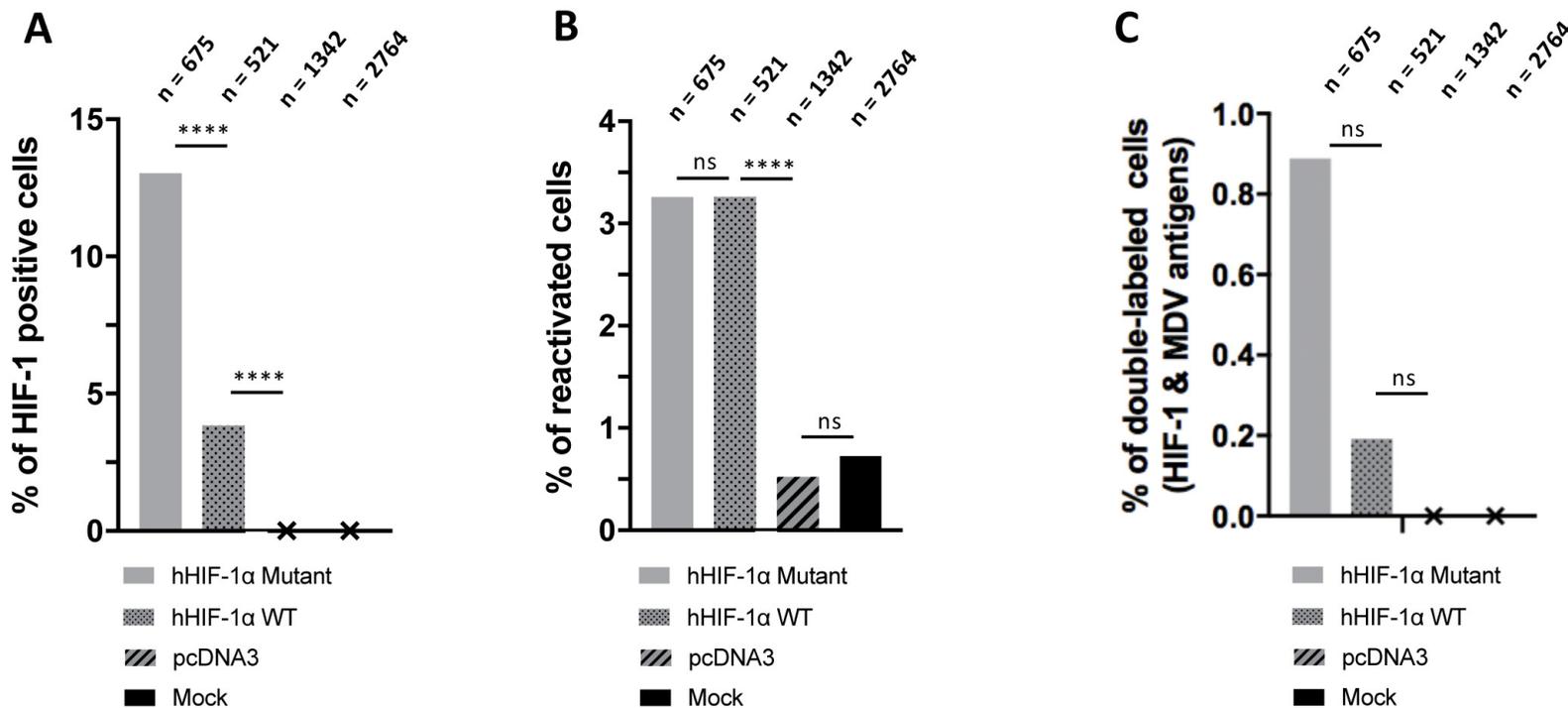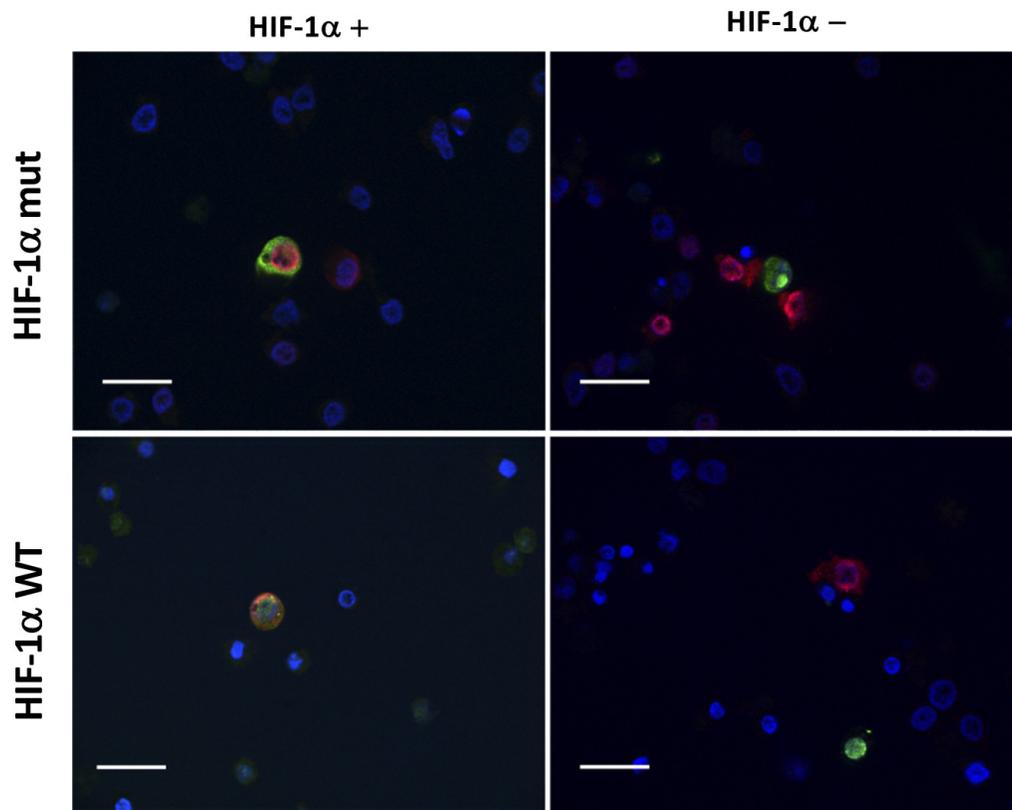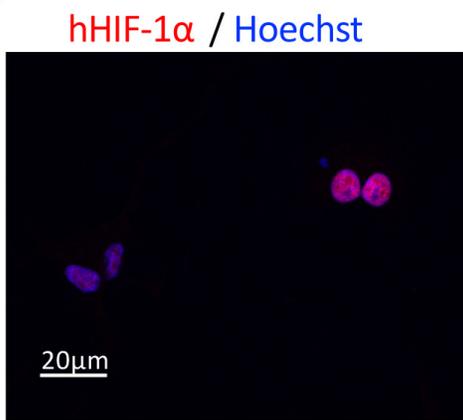
n = 675　n = 521　n = 1342　n = 2764

**** (between hHIF-1α Mutant and hHIF-1α WT)

**** (between hHIF-1α WT and pcDNA3)

% of HIF-1 positive cells

15

10

5

0

- ▨ hHIF-1α Mutant
- ▨ hHIF-1α WT
- ▨ pcDNA3
- ■ Mock

B

n = 675　n = 521　n = 1342　n = 2764

ns　****　ns

% of reactivated cells

4

3

2

1

0

- ▨ hHIF-1α Mutant
- ▨ hHIF-1α WT
- ▨ pcDNA3
- ■ Mock

C

n = 675　n = 521　n = 1342　n = 2764

ns　ns

% of double-labeled cells
(HIF-1 & MDV antigens)

1.0

0.8

0.6

0.4

0.2

0.0

- ▨ hHIF-1α Mutant
- ▨ hHIF-1α WT
- ▨ pcDNA3
- ■ Mock

D

Reactivated cells

HIF-1α +　　　HIF-1α −

HIF-1α mut

HIF-1α WT

HIF-1α ; **ICP4 - VP22** ; **Hoechst 33342**

Figure 9

A

hHIF-1α / Hoechst

20μm

B

○ w/o HIF-1α

● w HIF-1α

Figure 10

A

B